SISSA - SCUOLA
INTERNAZIONALE
SUPERIORE
DI STUDI AVANZATI
TRIESTE
Strada Costiera 11

ISAS - INTERNATIONAL SCHOOL FOR ADVANCED STUDIES

October 1984

TOROIDAL STARS

Thesis submitted for the degree

of

Master of Philosophy

CANDIDATE:

A.Lanza

SUPERVISORS:

Prof. M.A.Abramowicz

Prof. J.C.Miller

TRIESTE

ISAS - INTERNATIONAL SHOOL FOR ADVANCED STUDIES

October 1984

TOROIDAL STARS

Thesis submitted for the degree

of

Master of Philosophy

CANDIDATE:

A.Lanza

SUPERVISORS:

Prof. M.A.Abramowicz

Prof. J.C.Miller

INTRODUCTION

The first toroidal figures of equilibrium appeared in the literature in 1789 when Laplace constructed equilibrium configurations with such a topology for modeling Saturn's rings. In the recent years there has been a growing interest in such bodies since other astrophysical objects may be modeled through them (e.g. QSOs).

Although very recently Papaloizou and Pringle (1984) have shown the very important result that non self-gravitating torii around a central bodies possesses a global non-axisymmetric instability which acts on dynamical time scale, there are still good reasons for finding the equilibrium configuration of self-gravitating torii around massive objects in the framework of general relativity.

Papaloizou and Pringle use linear theory and it is not sure if including non-linearity we can have stabilizing effects. Moreover and more importantly it is not clear what physical effect will produce this instability. In both cases the answer could come from considering the full non linear perturbed equations and solve them numerically. In order to do that one should know the initial equilibrium configuration to start off.

Beyond this general considerations there are more specific astrophysical motivations that suggest to study that configuration.

The best model for QSOs and active galactic nuclei is that of a thick accretion disk around a black hole (for a complete review see Rees, 1984). The

luminosity of thick radiation pressure supported accretion disks is connected with their masses: low mas disks have toosmall surfaces to radiate at sufficient power. Moreover it has been shown (Abramowicz et al., 1982) that runaway instabilty (i.e. very fast mass exchange through the cuspe of the equipotential surfaces in the accretion disk model) is important for at least some realistic accretion disk models of active galactic nuclei. Both general relativity and self-gravity of the disk are important for discussing this instability.

Both effects are still important when a very close binaryneutron stars is considered. It has been suggested (Paczynski, 1984) that tidal forces can destroy the secondary. The material endowed of angular momentum may form a very thick disk whose mass is comparable with that of the primary.

Numerical calculations of dynamical relativistic collaps (Nakamura, 1981) have shown that during the collapse a ring forms due to shedding. It is very interesting from this point of view to see what value of a/m will have such a configuration.

It is not clear yet if the post-Newtonian dynamical instability at $e = 0.985$ in the MacLaurin spheroids leads to ring-like structure (Bardeen, 1971). Wong (1974) using Newtonian theory analized this conjecture and reached the conclusion that toroidal figures do not branch off from the MacLaurin spheroids. It is our opinion that the dynamical instability is a relativistic effect since only a post-Newtonian analysis has showed it.

All the mentioned reasons are good ones in our opinion for carrying out a study of general relativistic self-gravitating torii with or without a central body.

This thesis review all of those theorems and results obtained in the past which , in our opinion, are important to know in order to deal with rotating fluid masses with particular attention to torii.

The plan of the thesis is as follows. In Cap. I we discuss the theorems and results obtained in the framework of Newtonian theory for figures of equilibrium. Cap. II discuss them inside the theory of general relativitity. Cap. III contains a description of the main method used for that purpose.

C H A P T E R O N E

EQUILIBRIUM CONFIGURATIONS IN NEWTONIAN THEORY

§ 1. Some general results

Before going on to discuss some particular equilibrium configuration models we give here a small but important group of results that apply not only to rotating stars but they are so general that hold for any rotating fluid masses. A more complete and extensive exposition devoded for rotating stars can be found in the book by Tassoul (1978).

A rotating fluid mass is in hydrostatic equilibrium when the gravitational attraction is balanced by the outwards centrifugal and pressure forces. In cylindrical coordinates (r,z,φ) specifying rotation to be about the z axis, the hydrostatic equilibrium eqs. are the following

$$\frac{1}{\rho}\frac{\partial P}{\partial r} = -\frac{\partial \phi}{\partial r} + r\Omega^2 \tag{1.1}$$

$$\frac{1}{\rho}\frac{\partial P}{\partial z} = -\frac{\partial \phi}{\partial z} \tag{1.2}$$

where ρ, p, ϕ, and Ω are respectevely the mass density, pressure, gravitational potential and angular velocity. In addition to the above eqs., an equation of state and boundary condition must be specified.

The integration of eqs. (1.1) and (1.2) depends on the $p-\rho$ relation and on the rotation law. Great simplifications come if we assume that the fluid is a barotrope (p function only of ρ) and Ω function only of the distance r from the rotation axis. In this case the equations are integrable since it does exit a centrifugal potential.

Another simplification is provided by the Lichtenstein's theorem: rotating fluid masses for which the angular velocity does not depend on z have a plane of symmetry perpendicular to the axis of symmetry. This theorem, first proved for rigid-body rotation and uniform density (Lichtenstein, 1933) has been exten

ted even to differential rotation with non uniform density (see Stoeckly, 1965). When the potential is expanded using orthonormal polynomials (see later) this symmetry requires only even terms in the series.

All these results are derived only from the condition of mechanical equilibrium and are valid for any rotating systems. However they do not provide any idea on the distribution of angular momentum or the rotation law.

Constraints on the rotation law come from considerations of dynamical and thermal stability.

The usual approach to stability consists of considering small perturbations of the system and therefore studying the linearized time-dependent equations of hydrodynamics. Since the problem is linear the space variable $\underline{x}$ can be separated from the time so one can search for normal-mode solutions for the displacement of the form

$$\xi(\underline{x},t) = \xi(\underline{x},\omega)\, e^{i\omega t} \qquad (1.3)$$

The equations then will provide a dispersion relation from which one can study the sign of ω^2. It turns out that if $\omega^2 < 0$ the system will be unstable since the perturbation will increase in time, and if $\omega^2 > 0$ the system will be stable (the onset of instability occurs when $\omega^2 = 0$, which is called a neutral mode). In the first case we say that the system is dynamically or thermally unstable if the characteristic time-scale of the instability is of the order of the free-fall time $(G\bar{\rho})^{-1/2}$ or of the order of the Kelvin time GM^2/LR respectevely.

The main criterion is the Høiland one which states that a general non-isentropic configuration is dynamically stable if on each surface of constant entropy s the specific angular momentum $\ell = |r^2\Omega|$ must be increasing function of r

$$d\ell/dr > 0 \qquad (1.4)$$

In view of these results a model of a rotating configuration can be specified giving the total mass M, the total angular momentum J and a distribution of specific angular momentum satisfying the above criterion. Then fixing the mass one can construct a sequence of models with different amounts of rotation. Besides J, one is free to use another parameter which will charcterizes the main features along the sequence. In the case of a spheroid it is natural to use as a parameter the eccentricity since it gives an idea of how fast is the rotation. But the most convenient is provided by the ratio of rotational kinetic energy K to the gravitational potential energy

$$\tau = K/|W| \tag{1.5}$$

By virtue of the virial theorem, a rotating configuration in equilibrium composed of perfect fluid must satisfy

$$2K + W + 3(\Gamma - 1)U = 0 \tag{1.6}$$

where Γ is the adiabatic index and U is the internal energy. Since the last term must be positive otherwise the configuration would be radially unstable we have

$$2K \leq |W| \tag{1.7}$$

then

$$0 \leq \tau \leq 0.5 \tag{1.8}$$

This parameter gives us a qualitative idea about the concepts of slow and rapid rotation according to the inequalities

$K \ll |W|$ slow rotation

$K \sim |W|$ rapid rotation

§ 2. Equilibrium configuration of ellipsoidal shape.

Hydrostatic equilibrium of rotating stars has been studied using different approaches. As a first approximation one can assumethat the configuration is incompressible and rotates with the simplest rotation law, e.g. uniform rotation. These models can be thought of as a particular case of the more general centrally condensed polytropic bodies, rotating with a differential law. Making this generalization one can divide the approaches used so far into four groups. The first one adopts models in which the equipotential surfaces are level surfaces of tractable coordinate systems. This is applied to homogeneous and uniformly rotating bodies no matter how rapid is the rotation. The second is a modification of the first and treats slowly rotating objects whose equipotential surfaces deviate only slightly from simple surfaces (Chandrasekhar - Milne expansion). The third group uses a variational method in which the changes of the parameters describing the model are chosen among the ones which minimize the total energy (Roberts, 1962). The fourth group uses the most straightforward approach, that is the direct integration of the partial differential equations of equilibrium. This method has no limitations and can study as precisely as desidered centrally condensed uniformly rotating or differential stars. Different numerical methods used for this purpose will be discussed in Cap.III.

Since, as we shall see, homogeneous uniformly rotating bodies share many properties with the differential polytropes, we discuss those first.

Consider a body with constant density, uniform rotation and ellipsoidal shape with semi axis lenghts a_1, a_2, a_3 parallel to the axes x_1, x_2 and x_3 of a Cartesian frame of reference corotating about the x_3-axis. The hydrostatic equilibrium eqs. (1.1) and (1.2) have to be solved simultaneousely with the Poisson equation, which in this case assume the form

$$\frac{\partial \phi}{\partial x_j} = 2\pi G\rho A_j x_J \qquad j = 1,2,3 \tag{1.9}$$

where

$$A_J = a_1 a_2 a_3 \int_0^\infty \frac{d u}{(a_j^2 + u)} \tag{1.10}$$

$$\Delta^2 = (a_1^2 + u)(a_2^2 + u)(a_3^2 + u) \tag{1.11}$$

Putting (1.9) into (1.1) and (1.2), integrating we get

$$p/\rho = \frac{1}{2}\Omega^2(x_1^2 + x_2^2) - \pi G\rho \sum_{j=1}^{3} A_j x_j^2 + \frac{p_c}{\rho} \tag{1.12}$$

Then the isobaric surfaces are given by

$$\left(A_1 - \frac{\Omega^2}{2\pi G\rho}\right) x_1^2 + \left(A_2 - \frac{\Omega^2}{2\pi G\rho}\right) x_2^2 + A_3 x_3^2 = \frac{(p_c - p)}{\pi G\rho^2} = \text{const} \tag{1.13}$$

Since the boundary of any configuration, by convention, is defined by the condition p = 0 it is an isobaric surface. Then, in order that the boundary of the ellipsoid

$$\frac{x_1^2}{a_1^2} + \frac{x_2^2}{a_2^2} + \frac{x_3^2}{a_3^2} = 1 \tag{1.14}$$

coincides with one of the surfaces defined by eq. (1.13) we have

$$a_1^2\left(A_1-\frac{\Omega^2}{2\pi G\rho}\right)=a_2^2\left(A_2-\frac{\Omega^2}{2\pi G\rho}\right)=a_3^2A_3 \tag{1.15}$$

and eliminating the Ω^2 terms

$$a_1^2a_2^2(A_1-A_2)+(a_1^2-a_2^2)a_3^2A_3=0 \tag{1.16}$$

or solving with respect $\Omega^2/2\pi G\rho$

$$\frac{\Omega^2}{2\pi G\rho}=\frac{a_1^2A_1-a_2^2A_2}{a_1^2-a_2^2}=\frac{a_1^2A_1-a_3^2A_3}{a_1^2}=\frac{a_2^2A_2-a_3^2A_3}{a_2^2} \tag{1.17}$$

which holds if $a_1\neq a_2$. Then inserting into (1.16), (1.17) the definition (1.10) of the A_Js' we find

$$(a_1^2-a_2^2)\int_0^\infty\left[\frac{a_1^2a_2^2}{(a_1^2+u)(a_2^2+u)}-\frac{a_3^2}{(a_3^2+u)}\right]\frac{du}{\Delta}=0 \tag{1.18}$$

also

$$\frac{\Omega^2}{2\pi G\rho}=\frac{a_2a_3}{a_1}(a_1^2-a_3^2)\int_0^\infty\frac{u}{(a_1^2+u)(a_2^2+u)}\,\frac{du}{\Delta} \tag{1.19}$$

and similar expressions in which a_1 is replaced by a_2 and vice versa. Since (1.18) can be satisfied in two ways it follows that under the assumptions made, two equilibrium configurations are possible, namely, the axisymmetric ($a_1=a_2$) MacLaurin spheroids and the triaxial ($a_1\neq a_2$) Jacobi ellipsoids. Another immediate result comes from (1.19): since the left hand side is not negative it must be $a_1\geq a_3$ or $a_2\geq a_3$ that is the rotation axis is always the smallest.

Consider first the MacLaurin spheroid. If we introduce the eccentricity

$$e=\sqrt{1-\frac{a_3^2}{a_1^2}} \tag{1.20}$$

eq. (1.19) can be written as

$$\frac{\Omega^2}{2\pi G\rho} = A_1 - (1-e^2)A_3 \tag{1.21}$$

where now, A_1 and A_3 are only functions of e

$$A_1 = \frac{(1-e)^{1/2}}{e^3}\sin^{-1}e - \frac{(1-e^2)}{e^2} \tag{1.22}$$

$$A_2 = \frac{2}{e^2} - \frac{2(1-e^2)^{1/2}}{e^3}\sin^{-1}e \tag{1.23}$$

The associated relevant quantities can also be computed

$$M = \frac{4}{3}\pi a_1^3(1-e^2)^{1/2}\rho \tag{1.24}$$

$$I = \frac{2}{5}Ma_1^2 \tag{1.25}$$

$$J = I\Omega \tag{1.26}$$

$$\tau = \frac{3}{2e^2}\left[1 - \frac{e(1-e^2)^{1/2}}{\sin^{-1}e}\right] - 1 \tag{1.27}$$

and a sequence of axisymmetric models can be constructed for all the various values of e (or τ) forming the socalled MacLaurin sequence.

Jacobi considered the case $a_1 > a_2 > a_3$. The resulting models are triaxial ellipsoids and on solving eq. (1.18) one discovers that they exist only in the range $\tau_b \leq \tau \leq 0.5$ ($\tau_b = 0.1375$). This means that only rapidly rotating configurations can have triaxial symmetry.

The main features of the two sequences are shown in Figs. 1 and 2. Figure 1 shows that the eccentricity is an increasing function of the parameter τ. In Fig. 2 the dimensionless quantities

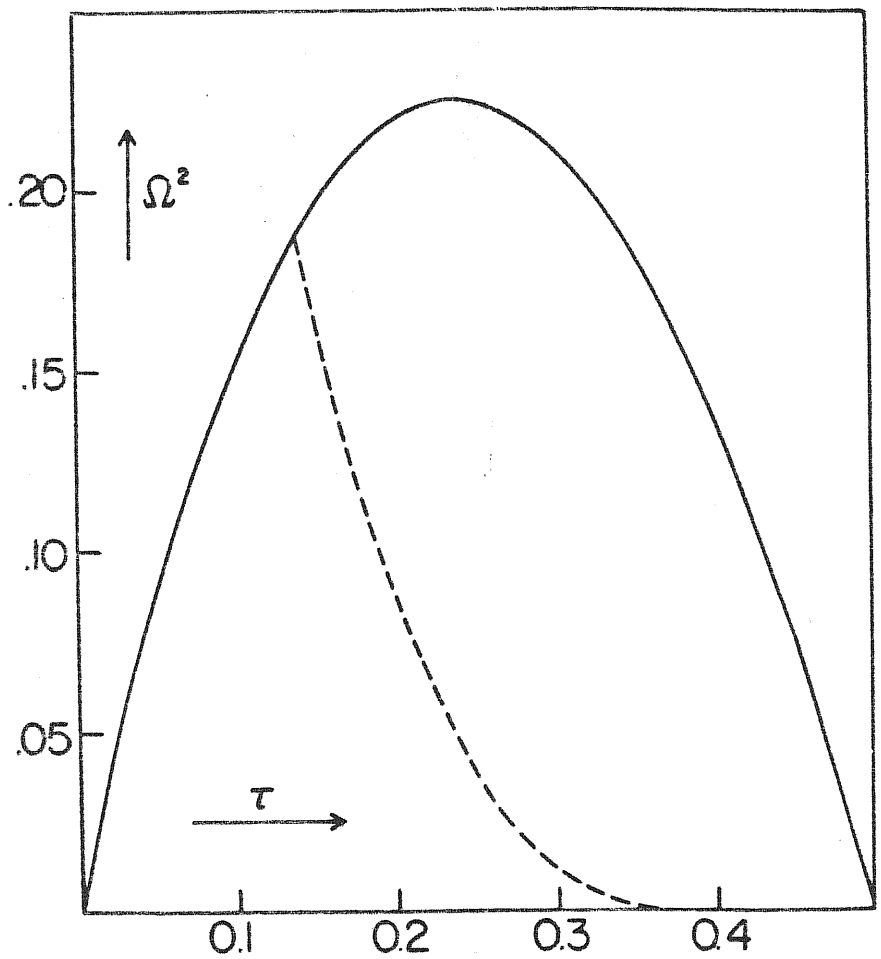

Figure 1. The squared angular velocity Ω^2 along the Maclaurin (*solid line*) and the Jacobi (*dashed line*) sequences, as a function of the ratio $\tau = K/|W|$. The unit of Ω^2 is $2\pi G\rho$. (See also Appendix D.)

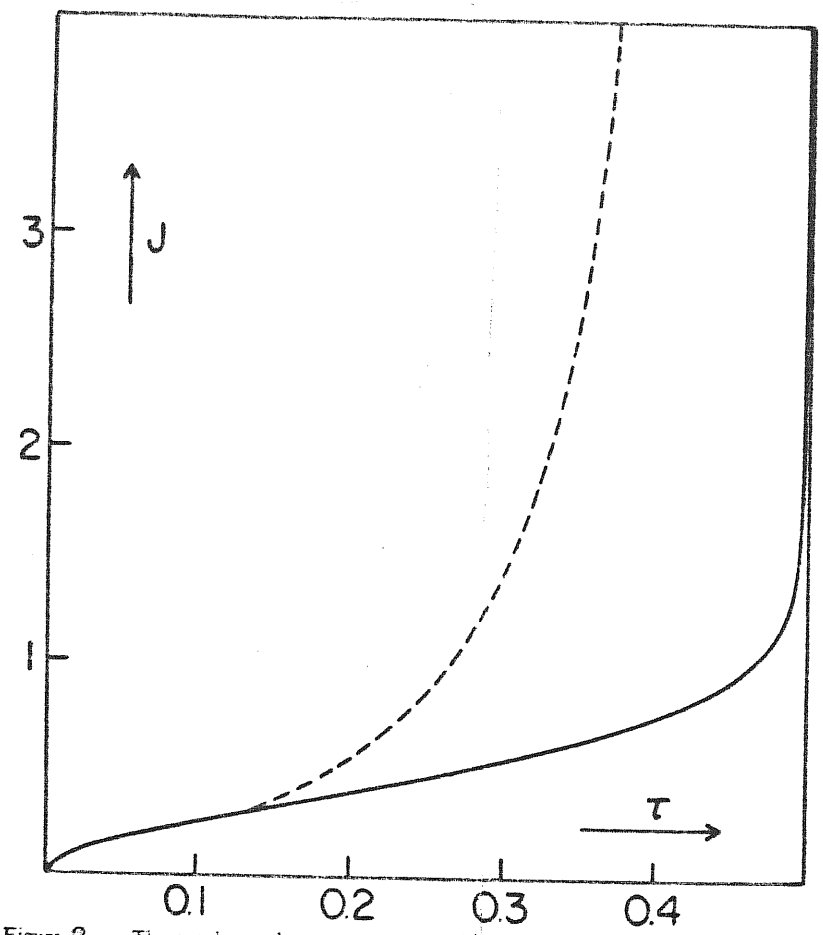

Figure 2 . The total angular momentum J along the Maclaurin (*solid line*) and the Jacobi (*dashed line*) sequences, as a function of the ratio $\tau = K/|W|$. The unit of J is $(GM^3\bar{a})^{1/2}$, with $\bar{a} = (a_1 a_2 a_3)^{1/3}$. (See also Appendix D.)

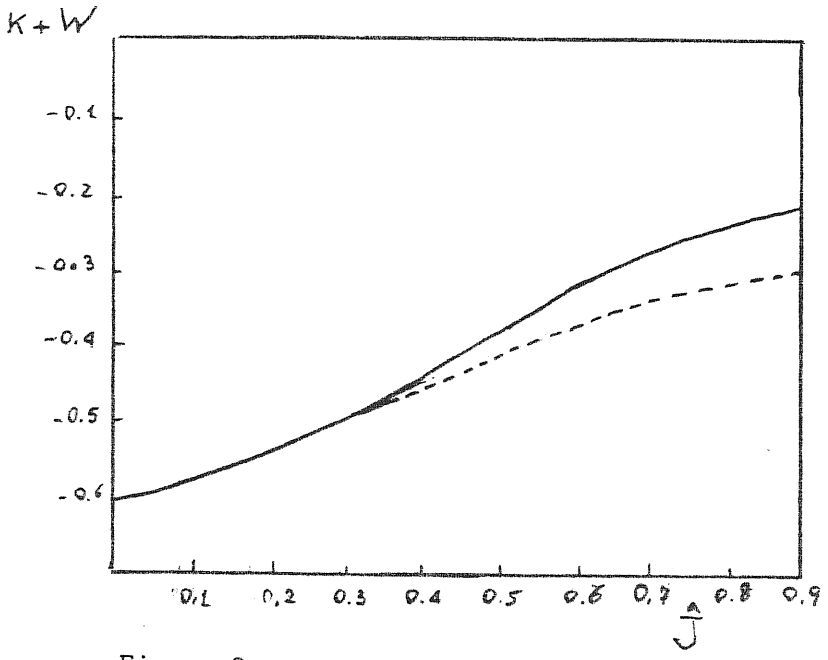

Figure 3

$$\hat{\Omega}^2 = \frac{\Omega^2}{\pi G \rho} \tag{1.28}$$

$$\hat{J} = \frac{J}{(G M^3 \bar{a})^{1/2}} \tag{1.29}$$

where $\bar{a} = (a_1 a_2 a_3)^{1/2}$, are plotted. The full lines refer to the MacLaurin sequence, whereas the dashed lines refer to the Jacobi one.

If we consider a star contracting slowly conserving M and J, $\hat{J}$ will increase monotonically as do τ and e, the object becomes progressively more oblate and it ends up as an infinitely thin disk. Moreover it can be seen that when $0 \leq \tau \leq \tau_b$ the MacLaurin spheroids are the only possible equilibrium configurations, whereas to each value of τ in the range $\tau_b \leq \tau \leq 0.5$ corresponds two figures of equilibrium.

In Fig. 3 the total mechanical energy K + W in units of $\frac{4}{3}\pi G \rho M \bar{a}^2$ is plotted against $\hat{J}$. The figure shows that the Jacobi ellipsoid has lower mechanical energy than the MacLaurin spheroid with the same M, J and volume V. Therefore if some dissipative mechanism reduces the total energy, the MacLaurin spheroid will evolve to the Jacobi ellipsoid beyond the point of bifurcation $\tau = \tau_b$. In order to check if this is the case one should solve the full set of hydrodynamical equations in which dissipation is included. Indeed, Press and Teukolsky (1978) integrating the Navier-Stokes Equations found that the MacLaurin spheroid slowly deforms into a Jacobi ellipsoid. But an insight into the problem comes from stability analysis. It can be shown that to the bifurcation point τ_b corresponds a neutral mode ($\omega^2 = 0$), but $\omega^2 > 0$ on both side of it. Moreover $\omega^2 = 0$, at $\tau = \tau_b$ is a double root and two sequences branch off the MacLaurin sequence at this point, namely, the Jacobi ellipsoids and the Dedekind sequence of triaxial ellipsoids whose overall shape is stationary relative to an inertial frame, although fluid circulates about the least axis. Now, if one includes viscous dissipation it can be shown

that ω^2 becomes negative beyond τ_b, and the imaginary part of ω is proportional to the viscosity. Then the perturbation increases slowly (on the viscous time-scale) and the MacLaurin spheroid evolves into a Jacobi ellipsoid minimizing energy. This is the so-called secular instability because it is slow and needs dissipation to operate. Including dissipation by gravitational radiation instead of by viscosity, Chandrasekhar (1970) has shown that there is again a secular instability driven by gravitational radiation reaction by which a MacLaurin spheroid evolves gradually to a Dedekind ellipsoid. Miller (1973) confirmed this result by studying numerically the evolution of the ellipsoidal figures including the effects of gravitational radiation.

Another point of onset of instability occurs beyond τ_b at $\tau = \tau_i = 0.2738$ along the MacLaurin sequence. Making the mode analysis at this point $\omega^2 = 0$, but ω^2 goes to negative values beyond τ_i no matter what physical process is going on. At this point the MacLaurin spheroids become dynamically unstable. It is interesting to note that the axis ratio is 3 : 1 at this point. As we shall see this ratio is found even for toroidal configurations at the onset of instability induced by beaded displacement.

The point of dynamical instability on the MacLaurin spheroid can be reached when viscosity and gravitational radiation reaction work togheter or when dissipative effects are neglected. Indeed, Lindblom and Detweiler (1977) discussed the combined effects on the stability of MacLaurin spheroids. They found thet when both dissipations are considered togheter those instabilities tend to cancel each other. This occurs because viscosity and gravitational radiation reaction cause different modes to become unstable. In particular, the mode which is unstable to radiation reaction is stabilized by viscosity. By this cancellation the onset of the secular instability can be delayed to a value of τ which depends on the ratio of the strenghts of the viscous and the gravitational forces. For a particular value of this ratio the stable

portion of the MacLaurin sequence can extend all the way to the point of the onset of dynamical instability.

When the dissipative effects are neglected ω^2 does not assume complex values and the axisymmetric configuration will follow the MacLaurin sequence till the point $\tau = \tau_i$ in which the spheroids become dynamical unstable with respect to non-axisymmetric perturbations that transform them to a barlike configuration.

A point of onset of dynamical instability occurs even in the Jacobi sequence when $\tau = 0.1628$. At this point a series of pear-shaped figures branches off the Jacobi sequence. These figures are secularly unstable and it is believed, though without any proof, that these figures will split into two detached masses giving rise to a binary system.

If we relax the hypothesis of homogeneity and uniform rotation then the problem of finding equilibrium configurations can be handled only numerically. James (1964) made the first calculations for uniformly rotating polytrpes whose equation of state is

$$p = k\rho^{1+\frac{1}{n}} = k\rho^{\Gamma} \tag{1.30}$$

where k is a constant depending on the entropy, n and Γ are the polytropic and adiabatic index respectevely. He used the analytical continuation method (see Cap. III) and constructed sequences of axisymmetric models with increasing rotation velocity, keeping constant n and the central density ρ_c. The range of the polytropic index covered by his calculations is $0 \leq n \leq 3$. He found that when $n > 0$ all the sequences terminate at $\tau = \tau_{max}$ depending on the value of n due to equatorial shedding since the effective gravity at the equator becomes zero. The most striking result he found is that for $n < 0.808$ there is always a non-axisymmetric bar mode instability at $\tau \cong 0.138$ irrespective of n if the sequence extends that far. For $n \geq 0.808$ the stars are always

stable up to the shedding point ($\tau_{max} \leq 0.138$). The above results suggest that uniformly rotating polytropes with $n \geq 0.808$ cannot store rotational energy to reach the point $\tau = 0.138$. So they are secularly and dynamically stable because they cannot rotate rapidly.

A different picture which resembles the MacLaurin sequence more, comes out from differential rotating polytropes. Stoeckly (1965) using a finite difference scheme (see Cap. III) constructed self-consistent models of axisymmetric differential rotating polytropes with n = 1.5. The rotation law he used was

$$\Omega(s) = \Omega_e \exp\left(- c \frac{s^2}{r_e} \right) \qquad (1.31)$$

where s is the distance from the rotation axis and r_e is the equatorial radius. This form allows some mathematical simplification since in this case the equation of hydrostatic equilibrium is integrable. Moreover the law (1.31) satisfies the Høiland criterion, which demands

$$c \frac{s^2}{r_e} \leq 1 \qquad \text{or} \qquad 0 \leq c \leq 1 \qquad (1.32)$$

Although, strictly speaking, values of c greater than 1 are not allowed, Stoeckly considered models in which the non-uniformity parameter c ranged from 0 to 0.15 in order to study models which ranged from uniform to rapid differential rotation. Figure 4 shows three models. The results indicate that for small values of c the sequences terminate with models with zero effective gravity at the equator (model B) confirming the result obtained by James. For rotation that is more non uniform the equidensity surfaces in the interior of the star assume a more elliptical shape (model G) and for $c \geq 0.67$ models pass from a cusped interior equidensity surface (model J) to a completely detached ring.

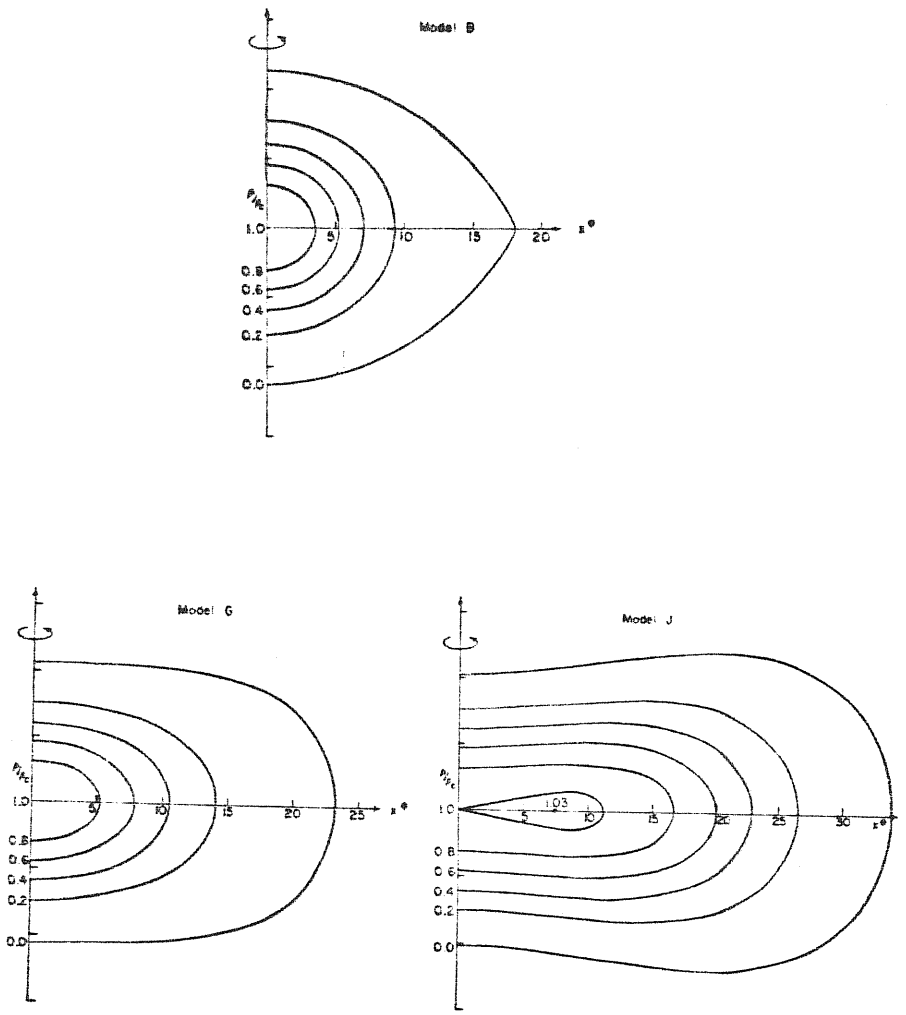

Figure 4

No stability analysis has been provided by Stoeckly.

More recent results have been obtained by Bodenheimer and Ostriker (1973) who considered more general polytropic sequences with index $0 \leq n \leq 3$. They used the self-consistent-field method presented by Ostriker and Mark (1968) in which the total potential (gravitational and centrifugal) is determined by potential theory from the density and velocity distributions, then the density distribution in equilibrium is determined algebrically from the derived potential (see Cap. III). The two steps are iterated until convergence is reached. Instead of giving as input the angular velocity distribution they specified the specific angular momentum ℓ as a function of a Lagrangian mass defined as the fractional mass contained in a cylindrical element inside the star. The assumed distributions are obtained by the formulae

$$\ell(m) = c_0 + c_1 (1 - m)^{\alpha_1} + c_2 (1 - m)^{\alpha_2} \qquad (1.33)$$

where the constants c_0, c_1, α_1 and α_2 are chosen to get the angular momentum distribution of a polytrope with uniform rotation at infinite radius. With this method they were able to compute sequence that resemble the MacLaurin ones in all important respects. Indeed, their sequences do not terminate at low e due to shedding and moreover their analysis of stability (Ostriker and Bodenheimer, 1973) indicates that the instability points on the MacLaurin sequence (secular at $e_s \sim 0.14$ and dynamical at $e \sim 0.27$) seem to be general features of more realistic models.

§ 3. Equilibrium configurations of self-gravitating torus with or without central body.

Spheroidal or ellipsoidal configurations are not the only axisymmetric equilibrium configurations that have been studied so far. Toroidal configurations have been considered partly because they are the next stage, in order of complexity, and partly for understanding astrophysical systems which surely show ring-shaped configurations like Saturn.

Two groups of systems have been taken into account: rings with and without central bodies. Basic work on the subject includes contributions of Laplace (1789), Maxwell (1885), Poincarè (1891)and Dyson (1893) who investigated the stability of rings with circular cross section and without central bodies.

We shall formulate the problem of finding the equilibrium of a self gravitating ring uniformly rotating about a central body as treated by Laplace. This description can also be found in Randers (1942).

As a first approximation the gravitational force acting at the surface of and inside the torus can be replaced by the force at the surface of and inside an infinite cylinder of the same cross-section and density. This approximation is correct since when the diameter of the torus goes to infinity, it degenerates to an infinite cylinder. It is not, however, allowed to replace the potential of the torus with that of the cylinder because the additive constant depends on the geometry of the torus. If we suppose that the ring is slender , i.e. minor axis << major axis ($d \ll R$) then the internal gravitational potential, in the case of circular cross section, is

$$V = -2\pi G\rho d^2 \left\{ \log \frac{8R}{d} + \frac{1}{2}\left(1 - \frac{r^2}{d^2}\right) \right\} \qquad (1.34)$$

where ρ is the density and r the distance from the rotation axis. In the case of elliptical cross section

$$V = -2\pi G\rho ab \left\{ \log \frac{16R}{a+b} + \frac{1}{2}\left(1 - \frac{\alpha x^2 + \beta y^2}{ab}\right)\right\} \tag{1.35}$$

where a and b are the axes of the ellipse in the plane of the torus and perpendicular to it respectevely; x and y are cartesian coordinates and

$$\alpha = \frac{2b}{a^2+b^2} \qquad \beta = \frac{2a}{a^2+b^2} \tag{1.36}$$

When a spherical body with mass M_c is put inside the ring the hydrostatic equilibrium equation gives, following a procedure similar to that for the MacLaurin spheroids

$$\frac{\Omega^2}{\pi G\rho} = \frac{4ab(a-b)}{(3a^2+b^2)(a+b)} \tag{1.37}$$

and

$$\frac{\Omega^2}{\pi\rho G} = \frac{M_c}{\pi\rho G R^3} \tag{1.38}$$

since the lhs is positive it must be that a > b, that is the torus is flatter in the equatorial plane. introducing a parameter γ such that

$$\frac{b}{a} = \frac{1-\gamma}{1+\gamma} \tag{1.39}$$

eq.(1.37) can be written

$$\frac{\Omega^2}{\pi G\rho} = \frac{\gamma(1-\gamma^2)}{1+\gamma+\gamma^2} \tag{1.40}$$

We see that $\Omega = 0$ when $\gamma = 0$ or $\gamma = \pm 1$. When $\Omega = 0$ it follows from (1.37)

that $R \to \infty$, then since $\gamma = -1$ has no meaning we can say that there are two possible cross sections for a ring in equilibrium at infinite distance from the central body, one circular with b/a = 1 ($\gamma = 0$) and one completely flat b/a = 0 ($\gamma = 1$). It can be seen from (1.38) and (1.40) that as the ring is posed to a closer distance from the central body, Ω increases and the circular cross-section becomes more and more elliptical, whereas the flat one becomes less and less elliptical. At a certain minimum distance D, the two cross-sections become identical and below this distance no equilibrium is possible. At this distance Ω is a maximum

$$\frac{\Omega_{max}}{\pi \rho \sigma} = 0.2172 \tag{1.41}$$

According to (1.38)

$$\frac{R_c^3}{R^3} \leq 0.1629 \frac{\rho}{\rho_c} \tag{1.42}$$

where R_c and ρ_c are the radius and density of the central body respectevely. Equation (1.42) tells us that the lower the density of the ring compared with the central body the larger is the radius of the ring compared to the radius of the central body.

Randers (1942) extended this study considering a spheroid as central body. Supposing that the ring is infinitely thin and that $R_c \ll R$ he found the almost obvious result that a purely spherical equilibrium is not possible, even when the body does not rotate, because of the attraction of the ring. Similarly, the additional outward attraction of the ring destroys the equilibrium for very flattened spheroids. He even studied for the first time the stability of such configurations. The results of his analysis shows that rings are stable to oscillations which expand or contract the radius, but

unstable against small changes in ellipticity of the cross-section. The flat equilibrium model will pass over to the configuration of nearly circular cross-section which is unstable against fragmentation.

A remarkable step in the study of self-gravitating rings has been made by Ostriker (1964b) who considered slender rings ($R \gg d$) with uniform rotation but with a polytropic equation of state. Using a perturbation tecnique, he was able to find a quite general solution of the Laplace equation which applies to any axisymmetric slender body. This method is quite similar to Chandrasekhar and Milne's one for rotationally distorted polytropes. In their work, the undistorted equilibrium configuration was spherically symmetric and the purpose was to find the centrifugal perturbing forces on a slowly rotating body. Ostriker considered as undistorted body a cylindrical polytrope whose structure was even found by him in an early paper (Ostriker, 1964a). Treating the rotation, the curvature of the cylinder and the presence of a central body as perturbations he was able to construct equilibrium models for different values of the polytropic index. The main results can be summarized in two statements. The equidensity surfaces of the ring are more distorted towards the center as the polytropic index increases (this seems obvious since as n increases the fluid becomes more compressible). The second result is that a central body forces the ring to rotate more rapidly. This is not surprising since if we put a body in the center of the ring the gravitational attraction will increase and only centrifugal forces which have opposite sign can compensate for it.

More recently Shuckhman (1982) studied the equilibrium and stability of a self-gravitating torus in the field of a large central mass. His model considered a special rotation law given by

$$\Omega = \Omega_0 \left(1 - \alpha \frac{r}{R}\right) \tag{1.43}$$

where Ω_0 and $\alpha \geq 0$ are constants. Using this law he found a relationship between the flattening and the amount of rotation α similar to that found by Laplace

$$\frac{\Omega_0^2}{4\pi G\rho_0} = \frac{\varepsilon(1-\varepsilon)}{(1+\varepsilon)(3-2\alpha+\varepsilon^2)} \qquad (1.44)$$

with $\varepsilon = b/a$ being the ratio of the axes of the elliptical cross-section. Here the maximum value of Ω_0 depends on the parameter α .

The stability analysis was mainly made considering radial perturbations. Two types of disturbances have been considered: those which are symmetric or antisymmetric about the outer surface of the torus. Only the symmetric perturbations have been found to be unstable. The instability may be dynamical, or it may be secular if dissipative processes are present. Non radial perturbations with azimutal wavelength much greater than the scale of the cross-section have been considered as well. It is found that if the torus is very flat these perturbations will give rise to any instabilities.

As far as toroidal configurations without central bodies are concerned the paper by Dyson (1893) represent the starting point. He considered toridal figures of equilibrium in which he expanded all the physical quantities in power series of the aspect ratio (R/d). He showed that when the aspect ratio exceeds 3, tori are unstable against beaded (or sausage) displacements in which the torus is thicker in same meridians but thinner in others.

A reexamination of these toroidal figures of equilibrium has been considered by Wong (1974) who was motivated by the conjecture of Chandrasekhar (1965,1967) and Bardeen (1971) that toroidal sequences branch off from the MacLaurin sequences due to instability excited by the post-Newtonian effects of general relativity. Wong constructed self-consistent equilibrium configurations for homogeneous and uniformly rotating tori using a method

that we will briefly describe here. He started with a torus with circular meridians whose potential was obtained in an early paper (Wong, 1973) as follows. All the relevant physical quantities are computed by separating them into two factors, the first is the quantity relative to a spherical body of the same mass M and density ρ while the second is a geometrical factor which takes into account the deviation from the spherical symmmetry. In particular, the gravitational energy, the rotational energy and the total energy are written respectevely as

$$E_m = E_m^{\circ} g_m \tag{1.45}$$

$$E_r = E_r^{\circ} g_r \tag{1.46}$$

$$E = E_m^{\circ} g_t \tag{1.47}$$

where the symbol "o" refers to the associated quantities for the spherical body and g_m, g_r and g_t are the geometrical factors. Expressions for these can be found in the paper by Wong (1974). It is interesting for our discussion to define the parameter x

$$g_t = g_m + x g_r \tag{1.48}$$

which is a measure of the angular momentum of the torus and it is linked to the usual parameter τ by the relation

$$\tau = x \frac{g_r}{|g_m|} \tag{1.49}$$

Wong uses x as a parameter to describe the toroidal sequences. The result thus obtained was used as a trial solution for the self-consistent iteration. The resultant equilibrium shape determined by that potential will in turn determine a new equilibrium shape and so on. The iteration is done keeping the volume constant and it is repeated till convergences of the shapes are reached. Figure 5 shows the results of these self-consistent solutions for various values of x, the lenghts being measured in units of $R_o = (3M/4\pi\rho)^{1/3}$. We see that for x = 2.0 the meridian is circular. As x decreases centrifugal forces increase and the meridian becomes flatter. According to this calculation a limit is reached (x = 0.8438) below which toroidal figures of equilibrium do not exist. This picture is different from Dyson's one upon which Bardeen based his conjecture. Indeed Dyson's sequences start at a value of x = 0.917 at which point the MacLaurin spheroid becomes unstable. Figure 6 shows a comparison between energies for the MacLaurin sequence and the toroidal one. We can see that there are no common points either at x = 0.8437 or x = 0.917. Accordingly the toroidal sequence does not branch off from the MacLaurin one. All of the models discussed in this section are not very realistic because the hypothesis of homogeneity or solid rotation have never been relaxed together. It will be worthwhile to reexamine the toroidal figures of equilibrium for differentially rotating polytropic models. For doing that one should resort to numerical calculations using a self-consistent method. Moreover a full dynamical code which includes transport of angular momentum can answer the problem whether the toriodal sequence branches off from the MacLaurin one.

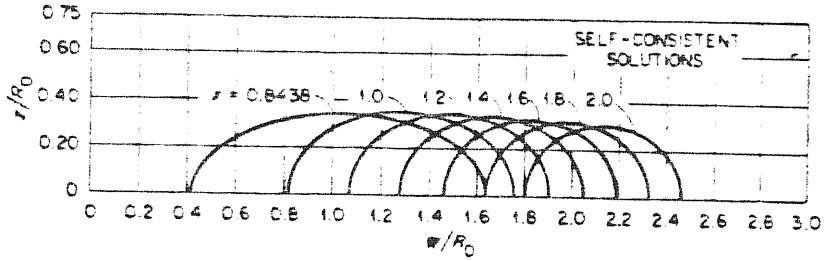

FIG. 5 —Meridian shapes of toroidal figures of equilibrium for various values of x obtained in a self-consistent manner. The z-axis is the axis of rotational symmetry.

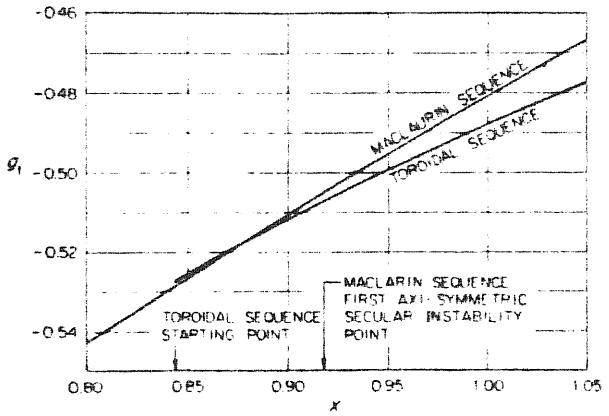

FIG. 6 —Comparison of the total energy for the Maclaurin sequence and the toroidal sequence. The toroidal sequence commences at x_t = 0.8437(5) while a Maclaurin spheroid becomes secularly unstable axially at x_s = 0.91761.

C H A P T E R T W O

ROTATING STATIONARY AXISYMMETRIC CONFIGURATIONS IN GENERAL RELATIVITY

§ 1. Equations and boundary conditions.

The space-time of a stationary axisymmetric configuration with rotation is endowed of two Killing vectors η^i and ξ^i which define the time coordinate t and the azimuthal coordinate φ, namely

$$\eta^i = \delta^i_t \qquad \xi^i = \delta^i_\varphi \tag{2.1}$$

where δ^i_j is the Kronecker's delta function. By transformation of the remaining two coordinates among themselves the line element can be reduced to the form (for the general theory of stationary axisymmetric configurations see Carter 1973 1979)

$$ds^2 = -e^{2\nu}dt^2 + r^2\sin^2\vartheta B^2 e^{-2\nu}(d\varphi - \omega dt)^2 + e^{2\zeta-2\nu}(dr^2 + r^2 d\vartheta^2) \tag{2.2}$$

The coordinate r, ϑ, φ are spherical at the asymptotically flat infinity. The metric functions ν, ω, B and ζ are only functions of r and ϑ since the symmetries of the space-time. The physical interpretation of these metric functions appears clear in the reference frame of a zero angular momentum observers (ZAMO) introduced by Bardeen (1970a). These observers find that $r\sin\vartheta\, B\, e^{-\nu}$ is the proper circumferential radius of a circle around the axis of symmetry. The function ω is the angular velocity that the ZAMO will acquire falling freely from infinity (dragging of the inertial frame) and $e^{-\nu}$ is the so-called "redshift factor" since it connects the proper time of the ZAMO with the coordinate time (proper time at infinity). The physical velocity v of the fluid relative to the local ZAMO is given in terms of the angular velocity of the matter relative to infinity

$$\Omega \equiv \frac{d\varphi}{dt} = \frac{u^{\varphi}}{u^{t}} \tag{2.3}$$

(where $u^{i} = (u^{t}, u^{\varphi}, 0, 0)$ is the four-velocity of the fluid) via the relation

$$v = (\Omega - \omega)\, r \sin\theta\, B\, e^{-2\nu} \tag{2.4}$$

Moreover since the metric function g_{oo} can have both negative and positive sign, wherever is $g_{oo} > 0$, no local observer with $\Omega = 0$ (stationary at infinity) can exist in such a region. This means that the inertial frame are not at rest with respect to infinity but are dragged round by the matter acquiring angular velocity relative to infinity equal to ω .

The Einstein's equations take a particularly simple form when they are projected onto the orthonormal tetrad of the ZAMO (Bardeen, 1970)

$$\tilde{\nabla}\cdot(B\tilde{\nabla}\omega) = \tfrac{1}{2} r^{2}\sin^{2}\theta\, B^{3} e^{-4\nu}\, \tilde{\nabla}\omega\cdot\tilde{\nabla}\omega + 4\pi B e^{2\beta-2\nu}\left[\frac{(\varepsilon+p)(1+v^{2})}{1-v^{2}} + 2p\right] \tag{2.5}$$

$$\tilde{\nabla}\cdot(r^{2}\sin^{2}\theta\, B^{3} e^{-4\nu}\tilde{\nabla}\omega) = -16\pi r \sin\theta\, B^{2} e^{2\beta-4\nu}\frac{(\varepsilon+p)v}{1-v^{2}} \tag{2.6}$$

$$\tilde{\nabla}\cdot(r\sin\theta\,\tilde{\nabla}B) = 16\pi r \sin\theta\, B\, e^{2\beta-2\nu} p \tag{2.7}$$

$$\begin{aligned}
\beta_{,\mu} = &-\left\{(1-\mu^{2})\left(1+r\frac{B_{,r}}{B}\right)^{2} + \left[\mu - (1-\mu^{2})\frac{B_{,\mu}}{B}\right]^{2}\right\}^{-1}\left[\left[\frac{1}{2}B^{-1}\left\{r^{2}B_{,rr} - \left[(1-\mu^{2})B_{,\mu}\right]_{,\mu} - 2\mu B_{,\mu}\right\}\cdot\right.\right. \\
&\cdot\left\{-\mu + (1-\mu^{2})\frac{B_{,\mu}}{B}\right\} + r\frac{B_{,\mu}}{B}\left[\frac{1}{2}\mu + \mu r\frac{B_{,r}}{B} + \frac{1}{2}(1-\mu^{2})\frac{B_{,\mu}}{B}\right] + \frac{3}{2}\frac{B_{,\mu}}{B}\left[-\mu^{2} + \mu(1-\mu^{2})\frac{B_{,\mu}}{B}\right] \\
&- (1-\mu^{2})r\frac{B_{,\mu r}}{B}\left(1 + r\frac{B_{,r}}{B}\right) - \mu r^{2}(\nu_{,r})^{2} - 2(1-\mu^{2})r\nu_{,\mu}\nu_{,r} + \mu(1-\mu^{2})(\nu_{,\mu})^{2} - 2(1-\mu^{2})r^{2}\times \\
&\times\frac{B_{,r}}{B}\nu_{,\mu}\nu_{,r} + (1-\mu^{2})\frac{B_{,\mu}}{B}\left[r^{2}(\nu_{,r})^{2} - (1-\mu^{2})(\nu_{,\mu})^{2}\right] + (1-\mu^{2})B^{2}e^{-4\nu}\left\{\frac{1}{4}\mu r^{4}(\omega_{,r})^{2} + \right. \\
&+ \frac{1}{2}(1-\mu^{2})r^{3}\omega_{,\mu}\omega_{,r} - \frac{1}{4}\mu(1-\mu^{2})r^{2}(\omega_{,\mu})^{2} + \frac{1}{2}(1-\mu^{2})r^{4}\frac{B_{,r}}{B}\omega_{,\mu}\omega_{,r} - \frac{1}{4}(1-\mu^{2})r^{2}\frac{B_{,\mu}}{B}\times \\
&\left.\left.\times\left[r^{2}(\omega_{,r})^{2} - (1-\mu^{2})(\omega_{,\mu})^{2}\right]\right\}\right]
\end{aligned} \tag{2.8}$$

In this equations $\mu = \cos\vartheta$ and $\underset{\sim}{\nabla}$ is the three-dimensional derivative operator in a flat three-space with spherical coordinates r, μ, φ. The fluid variable e and p are the total mass-energy density and the pressure measured in a frame that comoves with the fluid.

For studying rotating stationary axisymmetric configurations beside the Einstein's equations we have to consider the equations of hydrostatic equilibrium, an equation of state and the rotation law. The equation of hydrostatic equilibrium

$$T^{ij}{}_{;j} = 0 \tag{2.9}$$

with $T^{ij} = (e+p)u^i u^j + pg^{ij}$ can be written as

$$\underset{\sim}{\nabla}\phi + j\,\underset{\sim}{\nabla}\Omega - T(u^t)^{-1}\,\underset{\sim}{\nabla}s = 0 \tag{2.10}$$

In this equations the quantity ϕ is the energy required to inject a baryon from infinity into the star with zero angular momentum

$$\phi = \frac{e+p}{\mu}\,\frac{1}{u^t} \tag{2.11}$$

where n is the baryon number, j is the physical angular momentum per baryon,

$$j = \frac{e+p}{n}\,u_\varphi \tag{2.12}$$

T is the temperature defined as $T = (\partial\varepsilon/\partial s)_n$, and s is the entropy per baryon. The energy per baryon is

$$\mathcal{E} = -\frac{e+p}{n}\,u_t \tag{2.13}$$

A geometrical definition of the specific angular momentum is the following

$$\ell = \frac{J}{\mathcal{E}} = - \frac{u_\varphi}{u_t} \tag{2.14}$$

Using this definition the equation of hydrostatic equilibrium can be put in the form (Abramowicz et al., 1978)

$$\frac{\nabla_i p}{p+e} = - \nabla_i [\ln (u_t)] + \frac{\Omega \nabla_i \ell}{1 - \Omega \ell} \tag{2.15}$$

where ∇_i denotes covariant derivative. Then if the star is barotropic we can define a total potential

$$W = W_0 + \int_0^p \frac{dP}{p+e} \tag{2.16}$$

and use it for defining the boundary as an equipotential surface ("Boyer's condition", Boyer 1965). Moreover, in the isentropic case the surfaces Ω = const, ℓ = const, j = const, $\mathcal{E}$ = const and Φ = const inside the matter configuration have the topology of cylinders (von Zeipel's cylinders) and coincide (Abramowicz, 1974). Introducing then the "von Zeipel's" formulae

$$F = (1 - \Omega \ell) \exp \int_0^\ell (1 - \Omega \ell)^{-1} \Omega \, d\ell$$

we have

$$\Phi = \mathcal{E}_0 F$$

$$j = \mathcal{E}_0 \ell (1 - \Omega \ell)^{-1} F$$

$$\mathcal{E} = \mathcal{E}_0 (1 - \Omega \ell)^{-1} F$$

Then given a special form of the von Zeipel's formulae (i.e. a rotation law) we can easly solve the hydrostatic equilibrium equation.

Imposing the boundary conditions for the Einstein equations we should allow for the presence of a black hole, take into account asymptotically flatness at infinity and regularity on the axis of symmetry. At infinity e = p = 0, and the vacuum equations in the limit of weak field (see Chandrasekhar and Friedman 1972,for example) give

$$\nu = -\frac{M}{r} + O(r^{-2}) \tag{2.17}$$

which defines the gravitational mass

$$\omega = \frac{2J}{r^3} + O(r^{-4}) \tag{2.18}$$

which defines the total angular momentum, and

$$B = 1 + O(r^{-2}) \tag{2.19}$$

From (2.8) it then follows

$$\zeta = O(r^{-2}) \tag{2.20}$$

On the axis of symmetry local flatness implies that the radius of the circle around the axis $r \sin\vartheta\, e^{\zeta-\nu}$ must be equal to the proper circumferential radius $r \sin\vartheta\, B\, e^{-\nu}$, then

$$e^{\zeta} = B \tag{2.21}$$

The remaining boundary conditions are on the functions ν, ω and B at the inner edge. If no black hole is present then the metric functions have vanishing radial derivatives at r = 0 and vanishing gradients perpendicular to the axis of symmetry. When a black hole is present the inner boundary condition must be imposed on the horizon. Following Hawking and Carter(1973) the coordinate locus of the horizon can be made a surface of constant time and radius

$$r = h/2 \tag{2.22}$$

where h is a free parameter of the black hole. On the horizon $e^{2\nu}$ is zero ($\nu \to \infty$). The functions $r^2B^2e^{-2\nu}$ and $r^2e^{2\gamma-2\nu}$ must be regular positive of μ otherwise the intersection of the horizon with a space-like hypersurface have not regular two-geometry. Carter (1973) showed that necessary and sufficient conditions for regularity at the horizon are that $r\,B\,e^{-\nu}$ and ω must be regular functions of $\Delta = r+h^2/4r$ and μ in the neighbourhood of the horizon with

$$\frac{1}{r}\frac{\partial \omega}{\partial \theta} = 0 \tag{2.23}$$

With these boundary conditions the general vacuum solution for B is (Bardeen, 1973)

$$B(r,\mu) = \sum_{\ell=0}^{\infty} b_\ell r^\ell \left[1 - \left(h^2/4r^2\right)^{\ell+1}\right] T_\ell^{-\frac{1}{2}}(\mu) \tag{2.24}$$

where $T_1^{1/2}(\mu)$ are Gegenbauer polynomials. If ther is no matter between the horizon and infinity, asymptotically flatness implies $b_o = 1$ and $b_\ell = 0$ for $\ell > 0$. However if matter is present the b_ℓ should be adjusted to compensate for it.

The total mass and angular momentum of the system can be expressed in terms of the parameters of the black hole (Bardeen, 1973; Bardeen et al.,

1973)

$$M = M_H + \int \left\{ B e^{2\beta - 2\nu} \left[\frac{(\epsilon+p)(1+v^2)}{1-v^2} + 2p \right] + 2 r \omega_u \theta \omega B^2 e^{2\beta - 4\nu} \frac{(\epsilon+p)v}{1-v^2} \right] r^2 \omega_u \theta \, dr \, d\theta \, d\varphi \tag{2.25}$$

$$J = J_H + \int B^2 e^{2\beta - 4\nu} \frac{(\epsilon+p)v}{1-v^2} \, r^3 \omega_u^2 \theta \, dr \, d\theta \, d\varphi \tag{2.26}$$

where M_H and J_H are the mass and the angular momentum of the hole respectvely. The mass formulae can be written as (Smarr, 1972)

$$M_H = \frac{1}{4\pi} \kappa_H A_H + 2 \Omega_H J_H \tag{2.27}$$

where k_H is the gravitational acceleration of the ZAMO at the horizon

$$k_H = (e^{\nu})_{,r} \, e^{-\beta - \nu} \tag{2.28}$$

A_H is the surface area of the black hole

$$A_H = 2\pi \left(\frac{h}{2}\right)^2 \int_0^{\pi} \omega_u \theta \, d\theta \left[B \nu_{,r} \right]_{r=\frac{h}{2}} \tag{2.29}$$

and

$$\Omega_H = \omega)_{r=\frac{h}{2}} \tag{2.30}$$

is the angular velocity of the black hole. Hawking and Ellis (1972) and Carter (1973) have shown that k_H, A_H and Ω_H are constants on the horizon. The angular momentum of the Black hole is (Bardeen, 1973)

$$J_H = -\frac{1}{8} \left(\frac{h}{2}\right)^4 \int_0^{\pi} \omega_u^3 \theta \, d\theta \left[B^3 e^{-4\nu} \omega_{,r} \right]_{r=\frac{h}{2}} \tag{2.31}$$

If no black hole is present $M_H = J_H = 0$. When it is present two parameters characterize the boundary conditions on the horizon. They can be either the coordinate radius h/2 and the angular velocity Ω_H or the surface area A_H and J_H.

As we can argue from the above equations the problem of finding equilibrium configuration of rotating system in general relativity is far more complicated even in the simplest case of incompressible rigidly rotating fluid. The difficulty arise by the fact that no general solution is known for the exterior gravitational field. The Kerr solution can describe a very restricted class of axisymmetric objects. So one must resort to numerical methods or approximated tecniques. So far, four different lines of research have been followed. The first one considers the effect of relativity fairly small (post-Newtonian approximation, hereafter PPN) in which

$$\frac{GM}{Rc^2} << 1 \tag{2.32}$$

The second one considers only slowly rotating objects

$$R^2\Omega^2 << \frac{GM}{R} \tag{2.33}$$

The third and fourth ones apply to rapidly rotating fully relativistic models by using a variational principle method or by self-consistent-field calculations respectvely.

We will give here a very brief account of these lines of study concentrating on the papers we are more interested.

§ 2. Approximated approaches

In many cases where the densities of the stars are not very high, the relativistic corrections are quite small and the metric functions can be expanded in powers of $(1/c^2)$, truncating or retaining terms of the order $(1/c^2)^2$ according whether a first or a second order approximation is needed. Indeed, if one would like to take into account effects of gravitational radiation then the $2\frac{1}{2}$ approximation is needed. In a series of papers Chandrasekhar (1965, 1967, 1971) used this equations to study the effects of general realtivity on the classical MacLaurin spheroids and Jacobi ellipsoids. He showed that the principal relativistic correction is that the isobaric surfaces are pulled inwards at the equator and become less eccentric than predicted by Newtonian theory. Moreover, he found an axisymmetric instability at e = 0.985. This seems to be a PPN effect.

Bardeen (1971) reexamined the PPN form of the MacLaurin spheroid by using a different method. He gave a detailed discussion of the critical point at e = 0.985 . At this point, he suggested, a ringlike structure or a central bulge configuration may develop according whether dissipation transfers angular momentum inwards or outwards respectvely. Although Wong's Newtonian calculations do not confirme this conjecture, it will be worthwhile to carry out a full relativistic analysis as Bardeen himself suggested.

Another approximated method has been developed for those bodies (neutron stars, white dwarfs and supermassive stars) in which the centrifugal effects are small compared with the gravitational ones, as is stated in the condition (2.33). In this case the rotation can be treated as a small perturbation on an already known non-rotating configuration. The field equations are then expanded in powers of the angular velocity up to an order which includes general relativistic rotating effects (inertial frame dragging and deformation of the shape). Hartle (1967) derived the structure equations corrected to

second order in Ω.

Since the study of slowly rotating stars lead to an important group of results, which are confirmed by numerical calculations (see later) we will briefly describe here the method used.

The idea mainly consists of the following steps

a) A barotropic equation of state is specified

$$p = p(e). \tag{2.34}$$

b) Values of central density and angular velocity are chosen (this determines a unique equilibrium configuration).

c) A non-rotating stellar model is computed via the Tolman-Oppenheimer-Volkoff equation of hydrostatic equilibrium

$$\frac{dP}{dr} = -(e+p)\frac{(M+4\pi r^3 P)}{r(r-2M)} \tag{2.35}$$

$$\frac{dM}{dr} = 4\pi r^2 e \tag{2.36}$$

The metric that describes the spherically symmetric geometry has the Schwarzschild form

$$ds^2 = e^{-\nu(r)}dt^2 + \left(1-\frac{2M}{r}\right)^{-1}dr^2 + dr^2\left(d\theta^2 + \sin^2\theta\, d\varphi^2\right) \tag{2.37}$$

The only field equation is

$$\frac{d\nu}{dr} = -\frac{2}{e+p}\frac{dp}{dr} \tag{2.38}$$

d) When the equilibrium configuration is set into slow rotation the geometry changes and the perturbed metric is

$$ds^2 = -e^{\nu}\left[1+2(h_0+h_2P_2)\right]dt^2 + \frac{\left[1+2(m_0+m_2P_2)/(r-2M)\right]}{1-2M/r}\,dr^2$$

$$+ r^2\left[1+2(v_2-h_2)P_2\right]\left[d\theta^2+\sin^2\theta(d\varphi-\omega dt)^2\right] + O(\Omega^3) \qquad (2.39)$$

where $P_2 = P_2(\mu)=\frac{1}{2}(3\mu^2-1)$ is the Legendre polynomial of order 2; ω is the angular velocity of the local inertial frame; and h_0, h_2, m_0, m_2, v_2 are functions of r and proportinal to Ω^2. The expansion in even functions of μ is possible since the equatorial symmetry.

e) The "rate of dragging" is calculated solving the field equation for

$$\bar{\omega} = \Omega - \omega$$

$$\frac{1}{r^4}\frac{d}{dr}\left(r^4 j\,\frac{d\bar{\omega}}{dr}\right) + \frac{4}{r}\frac{dj}{dr}\,\bar{\omega} = 0 \qquad (2.40)$$

where

$$j(r) = e^{-\nu/2}\left[1-\frac{2M}{r}\right]^{1/2} \qquad (2.41)$$

f) The deformations of the shape of the star from the spherical symmetry are calculated solving the remaing field equations with respect to the perturbation factors m_0, h_0, h_2 and v_2.

Hartle and Thorne (1968) solved numerically the structure equations for modelling rigidly rotating neutron stars and white dwarfs whose matter was assumed to obey either the Harrison-Weeler (1965) equation of state or Tsuruta and Cameron (1966) V_γ equation of state. Figures 7 and 8 show the result of this calculations. We can see that the effect of rotation is not very large.

Those equations have been used for studying uniform slowly rotating configurations by Chandrasekhar and Miller (1974). The aim of studying

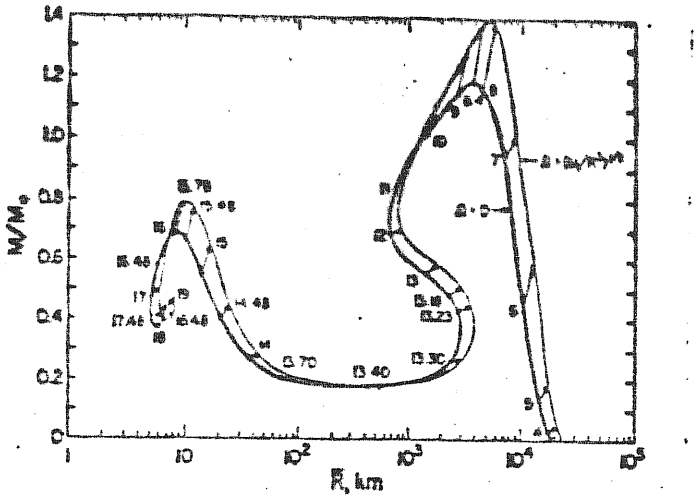

FIG.7. The results of Hartle and Thorne showing the effect of rotation on the curve of mass versus mean radius for configurations composed of matter obeying the Harrison-Wheeler equation of state. The thick curve shows the relationship for non-rotating models and the thin curve shows that for rotating models with $\Omega = (M/R^3)^{1/2}$. This is approximately the angular velocity at which mass shedding occurs and the method is not valid for such rapid rotation. However, for smaller values of Ω where the method is valid, the deformation of the mass-radius curve is simply smaller by a factor Ω^2R^3/M. The small arrows indicate the displacement, with increasing angular velocity, for configurations with the given central densities (the logarithm of the central density in g cm^{-3} is used as a parameter along the curves). To find the mass and mean radius of a configuration with a given central density and given angular velocity, one moves out along the appropriate arrow by the fraction Ω^2R^3/M of the total length of the arrow.

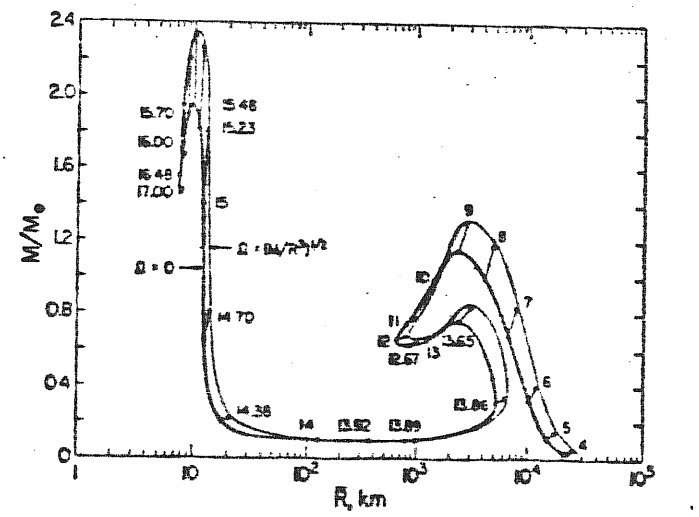

FIG.8. The effects of rotation on the masses and mean radii of configurations with the Tsuruta and Cameron V, equation of state. The format of this figure is the same as that of Fig.1.

homogeneous bodies is that to see which are the effects of general relativity on slowly rotating configurations, since stable homogeneous bodies can have radius R down to 9/8 of the Schwarzschild's radius R_s whereas in the case of more realistic equation of state the requirements of stability with respect to radial pulsations restrict the model to radii greater than 2.5 R_s (Chandrasekhar, 1964). Moreover, since they were interested to mimic a dynamic collapse their sequence was constructed for different values of R/R_s. The main results of these studies can be seen in figs. 9-11. In fig.9 the ellipticity ϵ of the body is plotted against R/R_s, we can see that ϵ does not increase monotonically during the contraction but reaches a maximum at $R/R_s \sim 2.3$ and then decreases again. What appears to be happening here is that non linear relativistic effects enable the inward gravitational forces to overcome the outward forces. Fig. 10 shows the $l = 0$ deformation of the bounding surface versus R/R_s. This figure indicates that the mean radius of slowly rotating body is smaller than that of a non-rotating body with the same central pressure. Figure 11 shows that as $R/R_s \to 9/8$ the ratio $QM/J^2 \to 1$ which is the value of this quantity required for the Kerr metric. Miller (1977) generalized this results to polytropic slowly rotating systems.

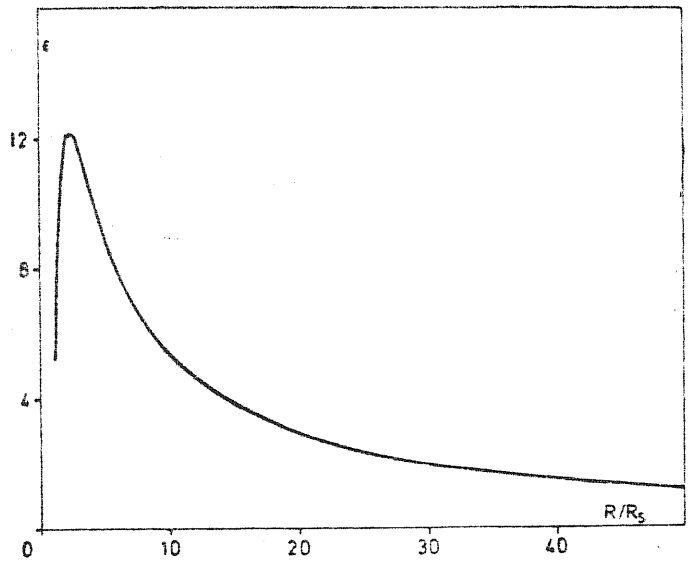

FIG. 9 *The ellipticity of the boundary: ϵ is plotted against R/R_S; ϵ is measured in the unit $G^2J^2/R_S^4c^2$.*

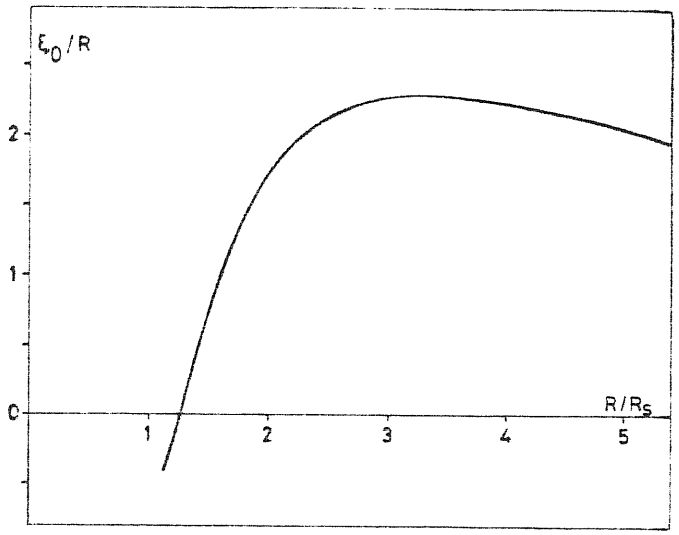

FIG.10 *The $l = 0$ deformation of the boundary: ξ_0/R is plotted against R/R_S; ξ_0/R is measured in the unit $G^2J^2/R_S^4c^2$.*

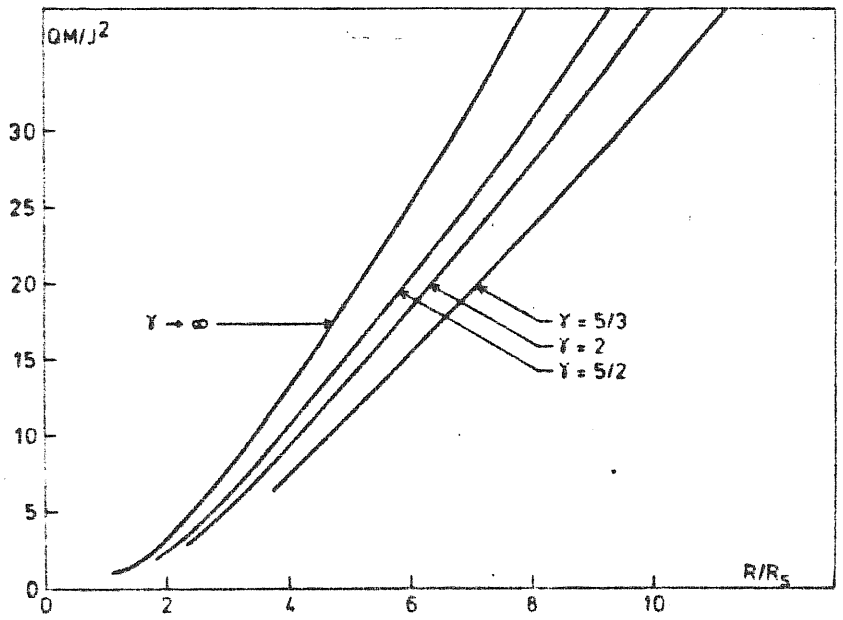

Fig. 11

§ 3. Rapidly rotating and full relativistic configurations

For studying the effects of rapid rotation and of general relativity altogether, the methods described above cannot be applied anymore. Then one should use numerical tecniques or variational principles.

The aim of these latter is to find an expression which, when extrimised under some constraints, can lead to equations and conditions which determine the equilibrium structure of the body in consideration.

For axisymmetric configurations in uniform rotation which are barotropic, Hartle and Sharp (1965, 1967) developed a variational principle. They gave expressions for the total mass-energy M, angular momentum J and baryons number N in terms of the metric functions and density distribution. Applying the variational principle an equilibrium model is found minimizing M under the constraints of specified J and N for all the star.

Abramowicz (1970) and Bardeen (1970b) independently developed a rather more general variational principle for perfect fluid configurations which can be differentially rotating and non-barotropic. Again here the equilibrium configuration is calculated extremising the total mass under the constrain that J and N are fixed for each ring of matter belonging to the configuartion in consideration. This was used by Abramowicz and Wagoner (1976) to compute neutron stars models.

When the self-consistent-field method is applied in general relativity the numerical problem becomes more complex since at each stage one should solve a set of four independent elliptical partial differential equations: one for each metric function. Relativistic calculations of this kind have been carried out first by Bardeen and Wagoner (1971) for disk configurations in which the

pressure vanishes (see later). Wilson (1972) considered differentially rotating polytropic bodies with index n = 3. His models are characterized by two quanti_ ties: α , the ratio of radius to thickness, and γ , the relativity factor previously used by Bardeen and Wagoner

$$\gamma = 1 - e^{\nu} \tag{2.42}$$

Varying these two parameters he constructed a sequence of models using an "ad hoc" distribution of density and angular momentum. He used a full 2-dimensional finite difference code for solving the exact field equations. Figures 12 and 13 show results of his computations. The binding energy $(M_o - M)/M_o$ (M_o is the rest mass density) versus γ is plotted in fig.12; we can see that, for fixed γ , the binding energy decreases as the configuration becomes more spherelike. In fig.13 contours of the metric conditions $g_{oo} = 0$ are plotted for $\alpha = 6$ and various values of γ . An ergotoroid is formed for $\gamma \geq 0.68$. In this region the dragging of the inertial frames is so strong that all the observers are forced to rotate. Mathematically, an ergoregion is the collection of points at which the metric function $g_{oo} > 0$, and hence at which the Killing vector ξ^t that is timelike at infinity is spacelike.

Bonazzola and Schneider (1974) developed numerical methods for constructing rotating fluid bodies with various pressure-density relations and various amount of flattening. Their method is somehow the general realtivistic version of Ostriker and Mark's one in which they used Green's functions tecniques for putting in integral form the Einstein's equations. However, this paper together

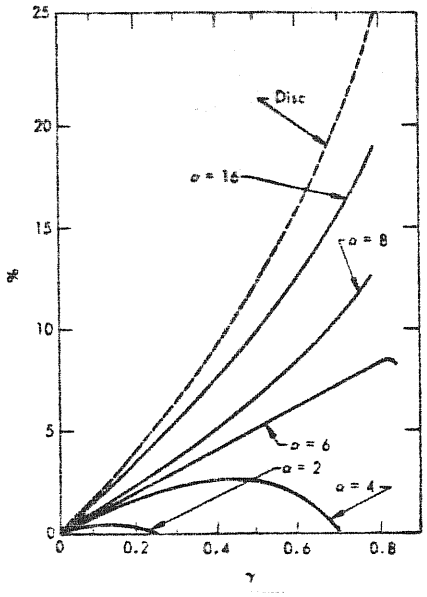
25
20
15
10
5
0
%
0
0.2
0.4
0.6
0.8
γ
Disc
α = 16
α = 8
α = 6
α = 2
α = 4

Fig. 12

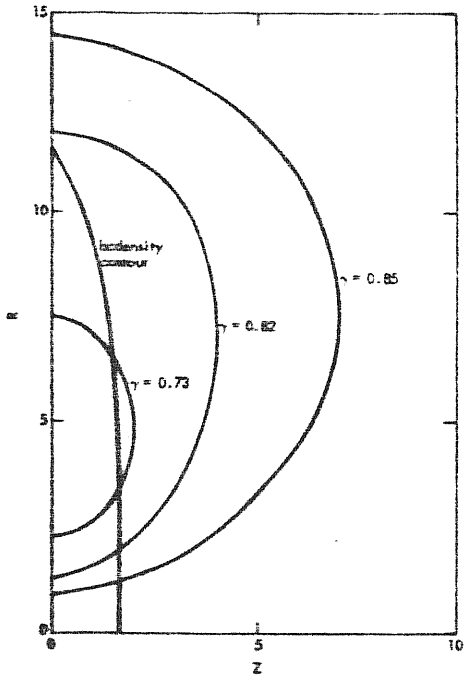
15
10
5
0
z
0
5
10
γ = 0.85
γ = 0.82
γ = 0.73

Fig. 13

with that of Wilson are opened to a certain amount of criticism. Wilson's method, for example, as we already said, places strong restrictions on the distribution of angular momentum. More importantly, Wilson approximates the boundary conditions garanteeing asymptotic flatness by certain "ad hoc" Newtonian-like conditions; and this might lead to significant inaccuracy in highly relativistic models. Bonazzola and Schneider's method contains artificial restrictions that cause it to break down in highly relativistic situations before many interesting rotational effects, such as the formation of ergoregions, may appear.

Very detailed sequences have been constructed by Butterworth and Ipser (1975,1976), Butterworth (1976,1979) using the general relativistic version of Stoeckly's method (see Cap. III). They used Neumann boundary conditions for the three elliptical field equations, which were developed through five orders in parameters (mass/radius) by recursive elimination of unknown coefficients in the expansions of the corresponding potentials.

In the first papers (Butterworth and Ipser, 1975, 1976) the code was applied to the construction of uniformly rotating homogeneous bodies which in certain cases exhibited interesting phenomenae. Specifically, it was found that unlike the Newtonian sequences of MacLaurin spheroids, fully relativistic sequences of uniformly rotating bodies terminate at points where centrifugal forces balance gravity at the equator (points marked "shed" in fig.14). Also, highly relativistic models with sufficient amount of rotation were found to develop regions within which observers must rotate with positive angular velocity $d\varphi/dt$ relative to infinity (points marked "ergo" in fig.14). For values of γ very low, numerical instabilities prevented to compute complete sequence with

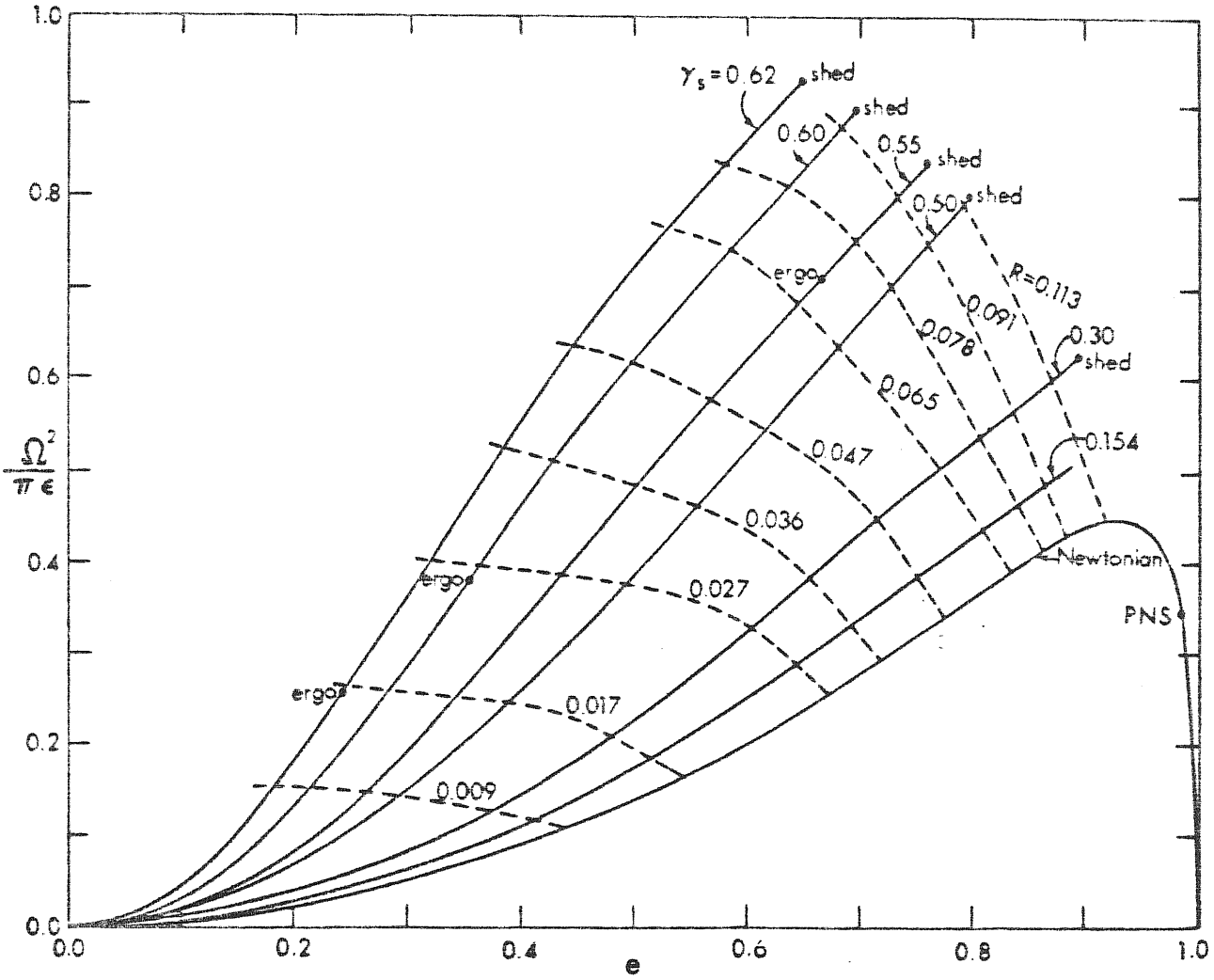

FIG. 14—A plot of the square of the uniform angular velocity, in units π times ϵ, versus the eccentricity (eq. [71]) of homogeneous bodies. The bottom solid curve is the Newtonian Maclaurin sequence. The other solid curves are relativistic sequences of fixed (rest mass) $\times \epsilon^{1/2}$. Each is associated with a particular value of γ_s, defined by eq. (66). The dashed curves are curves of constant rotation parameter R (eq. [65]). At the Newtonian point marked PNS, the post-Newtonian corrections to the Maclaurin spheroids become singular. At the points marked SHED, centrifugal forces balance gravity at the equator, and the sequences terminate. At the points marked ERGO, there appear regions within which observers must rotate relative to the distant stars.

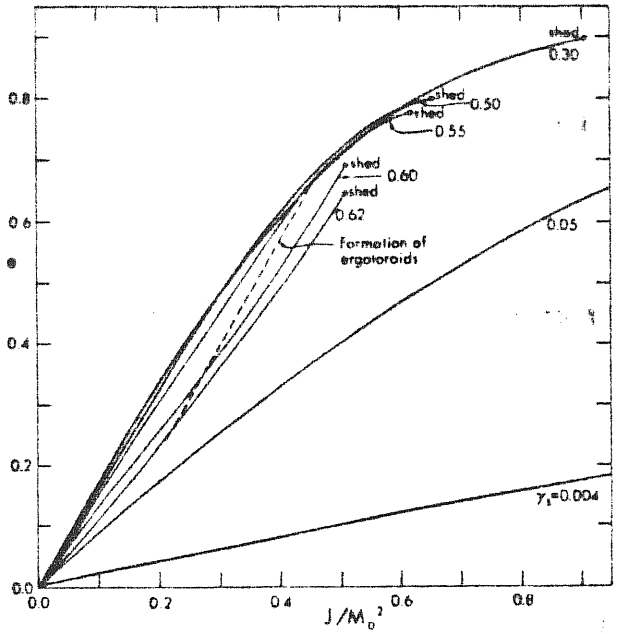

FIG. 15—A plot of eccentricity (eq. [71]) versus the ratio J/M_0^2, where J is the angular momentum and M_0 is the rest mass, for various relativistic sequences. The dashed curve marks the appearance of regions within which observers must rotate relative to the distant stars. At the points marked SHED, centrifugal forces balance gravity at the equator, and the sequences terminate.

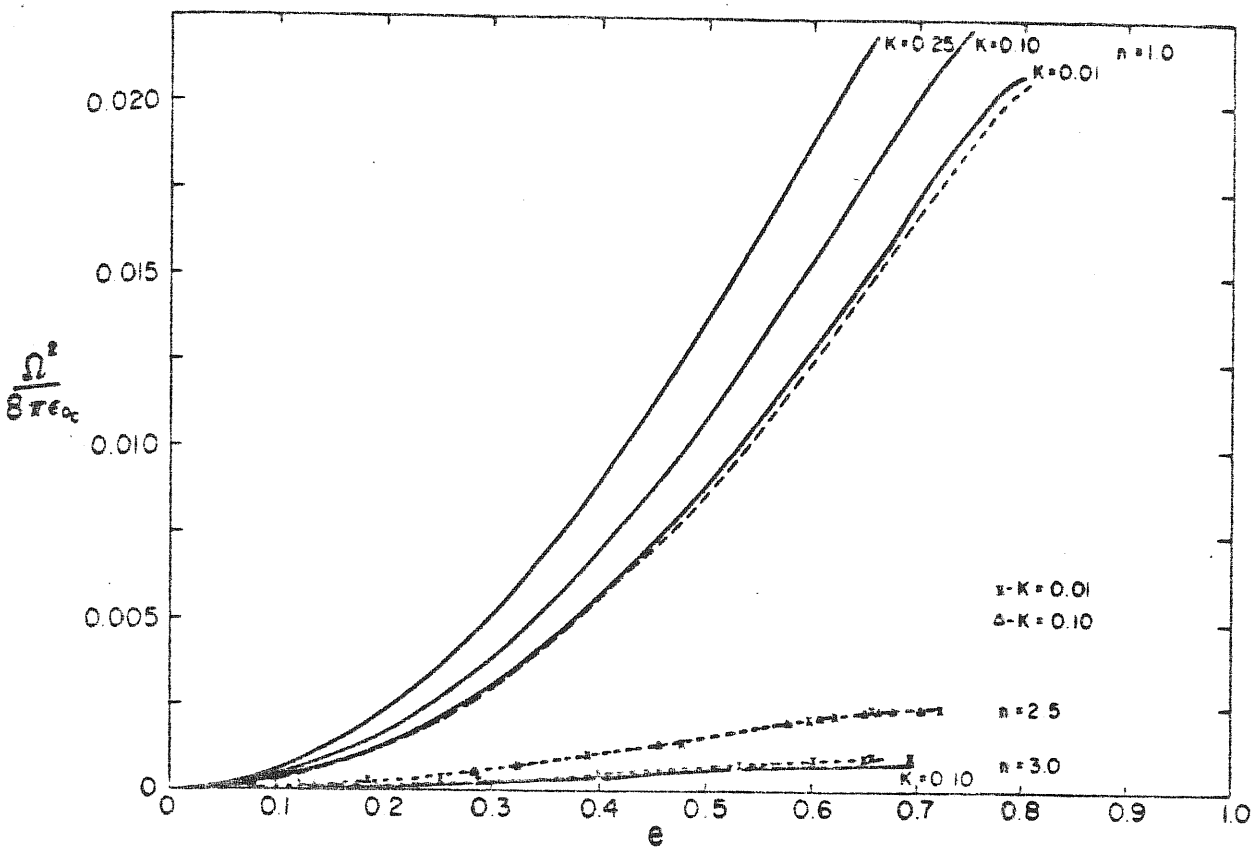

FIG. 16—A plot of the squared angular velocity of the matter, in units of 8π times central rest mass density, versus the eccentricity for pseudopolytropes of index n (*solid curves*) and for Newtonian polytropes of index n as computed by James (1964) (*dashed curves*). In some cases the solid curves are omitted for clarity and symbols appear at the data points.

termination points. In fig.15 the eccentricity versus J/M_o^2 is plotted. A body with $J/M_o^2 \leq 0.5$ reaches a maximum eccentricity ≤ 0.7 then moves downwards through states with smaller and smaller values of e. This confirm the result of Chandrasekhar and Miller already mentioned.

In a further paper Butterworth (1976) considered uniformly rotating pseudo-polytropes ($p \propto \varepsilon^{1+\frac{1}{n}}$). He did a comparison with the Newtonian computations made by James. In fig.16 we can see how close are the results between the Newtonian and relativistic case. The only difference is that for $n < 2.5$ relativistic objects are more spherical than their Newtonian counterparts of equal angular velocity and central rest mass density, while for $n > 2.5$ they are more flattened. No ergoregions where found for these objects.

A modification of the numerical method allowed Butterworth (1979) to compute solutions with angular velocity decreasing as a function of the angular momentum (high eccentricity). These models are important not only to extend the relativistic sequence further, but also to investigate the association between the termination points on relativistic sequences with the first axisymmetric secular instability of the MacLaurin spheroids which occurs after the maximum in angular velocity.

Figure 17 shows that sequences for $\gamma \lesssim 0.30$ have maxima in the angular velocity, whereas sequences with $\gamma \gtrsim 0.30$ terminate at the mass-shedding instability before a peak in the angular velocity is reached. The figure shows that these calculations are not very accurate since, for instance, the sequence with $\gamma = 0.004$ does not pass very near to the three points of Newtonian instabilities

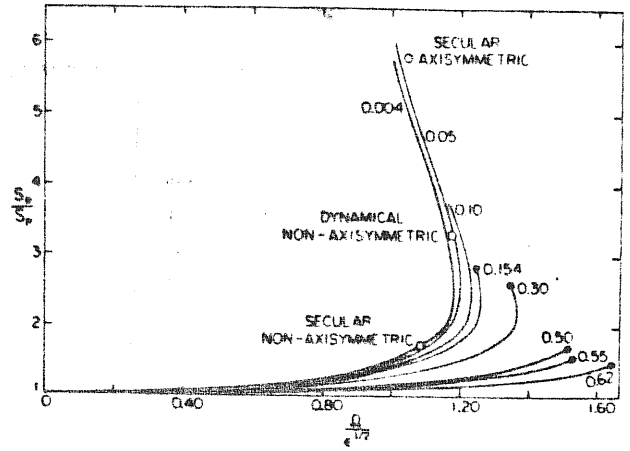

FIG. 17—The ratio of proper equatorial radius to proper polar radius versus the angular velocity of the fluid as seen by an observer at infinity in the unit of (mass density)$^{1/2}$. Open circles indicate the locations of instabilities of the Maclaurin spheroids. Large dots at the ends of some curves indicate termination points of those sequences. Curves are labeled by the applicable value of γ_e. Increments in the angular momentum are reduced progressively along the sequences, and in their latter parts are generally 1–3% for sequences up to $\gamma_e = 0.30$ and about 5% for $\gamma_e \geq 0.50$.

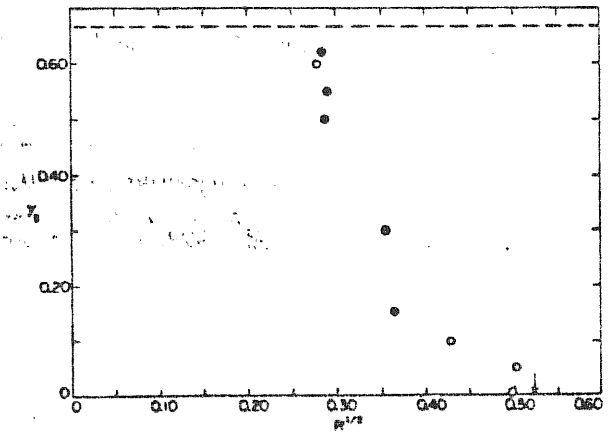

FIG. 18—The values of $R^{1/2}$ (see Fig. 3 for the definition) for the final member of each sequence—$\gamma_e = 0.004$, 0.05, 0.10, 0.154, 0.30, 0.50, 0.55, 0.60, and 0.62. Filled circles represent termination points of the sequences, open circles represent the values of $R^{1/2}$ for those sequences which for reasons of expense have not been continued further. The arrow indicates the location of the post-Newtonian singularity along the Maclaurin sequence at a value of $R^{1/2} = 0.52269$. The dashed line is drawn at the upper limit of $\gamma_e(\frac{1}{4})$ at which the central pressure of the spherical solution is infinite.

(open circle).

Figure 18, depicts the values of γ versus $R^{1/2}$ (=angular momentum*(mass density)$^{1/6}$/(rest mass)$^{5/3}$) for the final member of each sequence. Not all the data represent sequence termination points; open circles are simply the last models have been constructed for reasons of computer expense. From this figure is not clear whether the locus of the termination points of the relativistic sequences meets the point on the MacLaurin one at which the PPN corrections become singular (arrow in the figure) since at low γ the accuracy of the method is not high.

§ 4. Relativistic configurations of equilibrium with ring or disk shape

Detailed numerical solution of the Einstein's equations for the structure and gravitational field of uniformly rotating, infinitesimally thin disks which are supported radially entirely by centrifugal forces have been considered by Bardeen and Wagoner (1971).

Although the infinitesimally thin uniformly rotating disks are too unstable to fragmentation to be considered seriosly as realistic astrophysical configurations, this paper represent the starting point for the study of relativistic figures of equilibrium, since a very detailed tecniques for solving numerically the Einstein's equations for stationary and axisymmetric configurations have been carried out. The gravitational potential and the quantities characterizing the disk are expanded in powers of the relativistic parameter γ.

In the approximation of infinitesimally thin disk $p/e \ll 1$ and the pressure gradient force per unit inertial mass $\nabla p/(p + e)$ is significant only in the direction perpendicular to the plane of the disk where the infinitesimal thickness allows ∇p to become large enough. However, along the plane of the disk ∇p is finite and the pressure force is negligible compared with the gravitational and centrifugal forces. With this simplifications and considering the equatorial symmetry the field eqs. (2.7) has as solution

$$B = 1 \tag{2.43}$$

Putting $p = 0$ the others field equations become

$$\underset{\sim}{\nabla}^2 \nu = \frac{1}{2} r^2 \varpi u^2 \theta e^{-4\nu} \underset{\sim}{\nabla}\omega \cdot \underset{\sim}{\nabla}\omega \tag{2.44}$$

$$\frac{1}{r^2 \varpi u^2 \theta} \underset{\sim}{\nabla} \cdot \left(r^2 \varpi u^2 \theta \underset{\sim}{\nabla}\omega \right) = 4 \underset{\sim}{\nabla}\nu \cdot \underset{\sim}{\nabla}\nu \tag{2.45}$$

These equations are solved expanding all dimensionless quantities as power series in γ. For instance the metric function ν is written as

$$\nu(\xi, \eta; \gamma) = \sum_{n=1}^{\infty} \nu_n(\xi, \eta) \gamma^n \tag{2.46}$$

where ξ and η are oblate spheroidal coordinates. The coefficients ν_n are determined by the linear partial differential equations obtained putting the expansions in the field equations.

The equilibrium configurations are characterized by the rest mass M_o and the angular momentum J. Figure 19 shows that the ratio J/M_o^2 decreases monotonically as γ increases. For a given total angular momentum there is an upper limit to the rest mass or alternativaly for fixed M_o, there exist a minimum angular momentum for which equilibrium is possible. Moreover the fractional binding energy E_b/M_o is plotted against γ. The lack of a maximum suggests that uniformly rotating disks are stable aginst overall gravitational collapse.

Figure 20 shows how the angular velocity Ω increases to a limiting finite value as $\gamma \to 1$. The same figure shows that the ratio $M^2/J \to 1$ as $\gamma \to 1$. Fig.21 shows the development of ergoregion. Such regions first appears at $\gamma \sim 0.6$. Fig.22 shows the proper surface density against the dimensioless

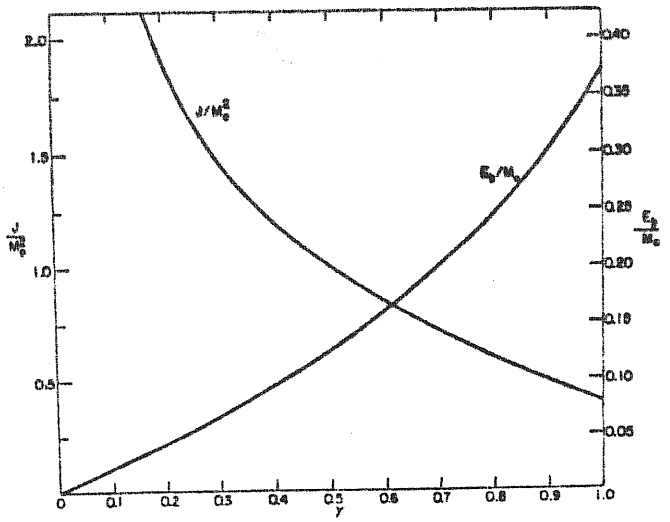

FIG 19—Angular momentum J and binding energy E_b as functions of the relativistic expansion parameter γ for a sequence of disk models with constant rest mass M_0. Note the different scales.

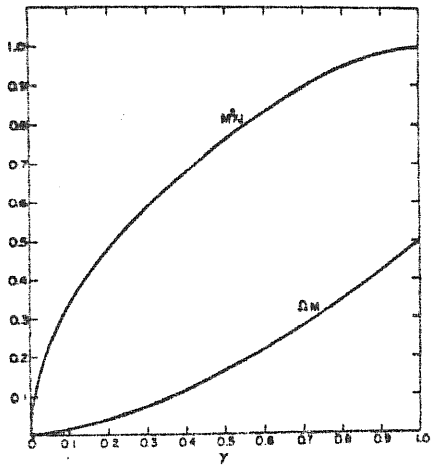

Fig. 20

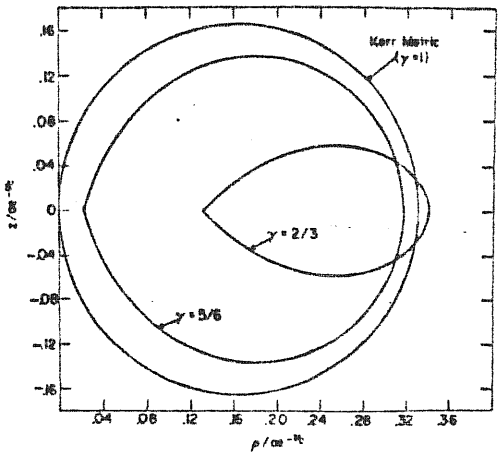

Fig. 21

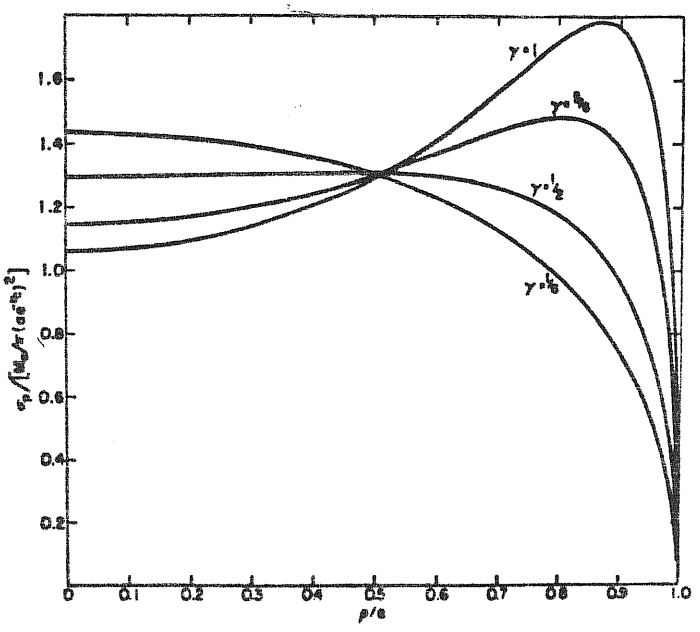

Fig.22

ratio of the rest mass m of the ring to its mean proper circunference R and by

$$\beta = h\,\omega_{(r=h/2)} = h\,\omega_H \tag{2.47}$$

respectevly. Thus the metric function ν is written as

$$\nu = \nu_0 + \sum_{m,n} \gamma^m \beta^n \nu_{mn} \equiv \nu_0 + \nu' \tag{2.48}$$

To first order in m and to second order in ω_H, he obtained a sequence of equilibrium configurations characterized by four parameters: the irrudicible mass $M_{ir} = (A_H/16\pi)^{1/2}$ of the black hole, R, m, and ω_H. The total mass and total angular momentum are

$$M = M_{ir} + m - \tfrac{1}{2} m\phi + 2 M_{ir}^3 \omega_H^2 - 12\,\omega_H m j \Psi \tag{2.49}$$

$$J = 4 M_{ir}^3 \omega_H - 8 m j (M_{ir}/R)^3 + m j' \tag{2.50}$$

where j is the angular momentum per unit mass of the ring given by

$$j = \left[M_{ir} R/(1 - 3 M_{ir}/R) \right]^{1/2} \tag{2.51}$$

moreover ϕ and Ψ are functions of M_{ir}/R. In fig.23 the main result of this study is given. There the mass curve for rotating black hole without ring is

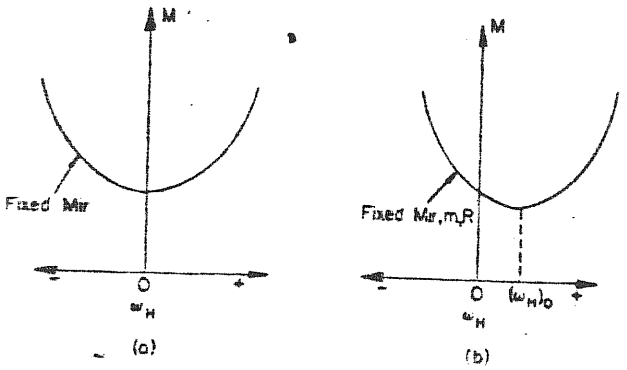

FIG. 23—Mass curve for rotating black holes. (*a*) For a vacuum Kerr black-hole the total mass M varies with ω_H (the angular velocity of the horizon) holding the irreducible mass M_{ir} fixed, and has a minimum at $\omega_H = 0$. (*b*) For a slowly rotating black hole with a stationary axisymmetric ring of matter around it, M varies with ω_H, holding fixed M_{ir} and the mass m and proper circumferential radius R of the ring. But here the minimum mass configuration occurs at $\omega_H = (\omega_H)_0 \neq 0$ (see text).

plotted against the angular velocity. The result suggests that the "Penrose process" (by which energy can be extracted from a rotating black hole) may be different for black hole-ring systems than for Kerr black holes. The suggestion derives from the fact that the total mass for the hole-ring configuratons has a minimum for non-zero value of w_4 . For this reason the black hole still posses an ergosphere in which particles can have negative energy (as seen from infinity); such an energy can be in principle extracted. This situation is in contrast with the Kerr case, where the minimum-energy configuration occurs precisely when the ergosphere vanishes ($w_4 = 0$) that is when further energy extraction is impossible. Thus a Penrose process can extract further energy from the system and this energy cannot comes only from the rotation of the hole, but even from the ring.

Abramowicz (1982) gives the metric for a self-gravitating ring around rotating black hole in the case of vorticity-free configurations. With the only assumption of vorticity-free ($\omega^2 = 0$) which means constant specific angular momentum since

$$\omega^2 = -\frac{1}{4}(1-\Omega\ell)^{-2}R^{-2}(\nabla_i\ell)(\nabla^i\ell) \tag{2.51}$$

$$R^2 \equiv \frac{\ell g_{t\varphi} + g_{\varphi\varphi}}{g_{t\varphi}^2 - g_{tt}g_{\varphi\varphi}} \tag{2.52}$$

he has been able to formally solve one Einstein equation reducing the number of unknown metric functions to only three.

C H A P T E R T H R E E

NUMERICAL METHODS

§ 1. Introduction

In this chapter we will discuss the main numerical methods that have been used in the past for computing equilibrium configuration in general, concentrating more on those developed by James (1964), Stoeckly (1965) and Ostriker and Mark (1968). Although all of them have been constructed for studying Newtonian configurations, we shall discuss the Stoeckly's one in the general relativistic version developed by Butterworth and Ipser (1976), since we are more interested in relativistic configurations.

The aim of these method is to give a tool for solving the field equations (Poisson or Einstein ones) consistent with a given distribution of matter. This problem can be solved by using an iterative procedure which consists in two steps: the "potential step" in which the field equations are solved for a given distribution of density and the "equilibrium step" in which a new distribution of density is computed from the previously potential.

The "potential step" is the more difficult one since the field equations are elliptical and they should be solved under both inner and outer boundary conditions. In general these are not known in advance and very often they are provided by algebraic or differential equations.

The general approach to this problem is that of the application of the finite difference calculus transforming the partial differential equations into finite algebraic ones. By using this approach a function is transformed into a vector of finite dimensions, a differential operator into a matrix operator and differential equations into matrix equations. As simple example let's consider the Poisson equations for one dimension only

$$\frac{d^2\phi(x)}{dx^2} = \rho(x) \qquad (3.1)$$

where $\rho(x)$ is the known source function and $\phi(x)$ is the unknown potential. If in an equally spaced grid with step size Δ, the differential operator d^2/dx^2 is approximated by

$$\frac{d^2f}{dx^2} = \frac{f_{i+1} - 2f_i + f_{i-1}}{\Delta^2} \qquad 1 \le i \le J \qquad (3.2)$$

where J is the total number of grid points, then eq. (3.1) can be written as

$$\phi_{i+1} - 2\phi_i + \phi_{i-1} = \Delta^2 \rho_i \qquad (3.3)$$

This holds in all the grid. Assuming that the boundary conditions are such that

$$\phi_1 = w_1 \qquad (3.4)$$

$$\phi_J = w_J \qquad (3.5)$$

then eq. (3.3) forms a set of simultaneous linear equations

$$\begin{aligned} \phi_1 &= w_1 \\ \phi_1 - 2\phi_2 + \phi_3 &= \Delta^2 \rho_2 \\ &\cdots\cdots \\ \phi_{J-2} - 2\phi_{J-1} + \phi_J &= \Delta^2 \rho_{J-1} \\ \phi_J &= w_J \end{aligned} \qquad (3.6)$$

which can be written in compact form

$$\underline{A}\ \underline{\phi} = \underline{w} \tag{3.7}$$

where $\underline{\phi}$ and $\underline{w}$ are colunm vectors and $\underline{A}$ is the matrix of the coefficients which in the case of one dimensional problem is tri-diagonal so special tecniques can be applied for solving eq. (3.7).

It is possible to generalize the above outlined method to two or more dimensions. In the case of two dimensions the functions must be replaced by matrixes increasing so the necessary memory by a factor given by the number of grid points chosen for the second dimension. This factor comes even in the number of operations needed increasing the computational time required. Moreover the matrix of the coefficients is not in general tri-diagonal even though it is "sparse", i. e. very few of its elements are non zero, the tecniques used them are more involved than for the tri-diagonal ones.

Problems of storage and of computational time can be avoid if the original problem of solving the Poisson equation is posed in a different way. This will be the case if one uses power series (e.g. James, 1964; Ostriker and Mark, 1968) to represent variations of the physical variables or if one uses a semidirect integration method (Stoeckly, 1965).

§ 2. Analytical continuation

Tis method essentially reduce the boundary value problem to a Cauchy one by using the fact that the potential is an analytical function of the radial coordinate in the interior of the body in consideration. James (1964) using this method solved the structure of a uniformly rotating polytropic system. In this case the Poisson equations can be written as+

$$\xi^{-2}\frac{\partial}{\partial\xi}\left(\xi^2\frac{\partial\psi}{\partial\xi}\right)+\xi^{-2}\frac{\partial}{\partial\mu}\left[(1-\mu^2)\frac{\partial\psi}{\partial\mu}\right]=-\rho' \tag{3.8}$$

where

$$\rho'=\rho/\rho_c=\Theta^n \tag{3.9}$$

$$\xi=r/a \qquad a^2=\frac{(n+1)K}{4\pi G\rho_c^{1-1/n}} \tag{3.10}$$

$$\psi=\frac{\phi}{(n+1)K\rho_c^{1/n}} \tag{3.11}$$

$$\Theta'=\psi+\frac{\Omega^2}{2(n+1)K\rho_c^{1/n}}r^2(1-\mu^2) \tag{3.12}$$

are the dimensioless quantities used and $\mu=\cos\theta$. The configuration under study is divided in three different regions . In the first one (region 1) the potential ψ is expanded in power series of ξ about $\xi=0$. In region 2 this expansion is extended by analytical continuation to $\xi=\xi_p$, where ξ_p is the polar radius of the configuration. Region 3 is the surface region in which $\xi_p\le\xi\le\xi_e$ with ξ_e being the equatorial radius. In this region ψ and ρ' are not analytical functions of ξ and it is used a different expansion.

+ Here the sign of the potential is opposite than that defined before.

In region 1, ψ and ρ' are expanded as

$$\psi = \sum_{ij} A_{ij} \xi^i P_j(\mu) \tag{3.13}$$

$$\rho' = \sum_{ij} B_{ij} \xi^i P_j(\mu) \tag{3.14}$$

where P_j are Legendre polynomials and A_{ij}, B_{ij} are coefficients to be determined. Imposing the boundary conditions at $\xi = 0$

$$\psi = 1 \tag{3.15}$$

$$\frac{\partial \psi}{\partial \xi} = 0 \tag{3.16}$$

from (3.13) we get

$$A_{oj} = \delta_{oj} \tag{3.17}$$

$$A_{1j} = 0 \quad . \tag{3.18}$$

A_{ij} and B_{ij} are related each other throughout the relation

$$\left[i\,(i+1) - j\,(j+1) \right] A_{ij} = - B_{i-2,j} \tag{3.19}$$

which is obtained by putting (3.13) and (3.14) into (3.8). Moreover according to Lichtenstein's theorem the configuration must have equatorial symmmetry. This means that

$$A_{ij} = B_{ij} = 0 \tag{3.20}$$

for odd iand j. In addition they vanish when $i < j$. The coefficients B_{ij} are determined as follows. Write the expansion (3.14) in a different way

$$\rho'(\xi,\mu) = \sum_i \rho_i'(\mu)\,\xi^i \tag{3.21}$$

where

$$\rho_i'(\mu) = \sum_j B_{ij} P_j \tag{3.22}$$

and by the orthogonality of the Legendre polynomials

$$B_{ij} = (j + \tfrac{1}{2}) \int_{-1}^{1} \rho_i'(\mu)\, P_j(\mu)\, d\mu \tag{3.23}$$

Since we know the values of A_{oj} and A_{1j}, using (3.12) and (3.9) we may determine the values of ρ_0' and ρ_1'. Then using an eleven points Gauss-Legendre quadrature eq. (3.23) will give the values of B_{oj} and B_{1j}. This in turn will be used to determine A_{2j} via (3.19) and so on. Equations (3.17)÷(3.20) determines then all coefficients A_{ij} for $i \neq j$. When $i = j$ eq. (3.19) is satisfied for any value of A_{ii}. Thus any set of coefficients A_{ii} determines a solution of (3.8).

The μ-wise expansion in (3.13) and (3.14) is terminated with the term $P_{10}(\mu)$, whereas the ξ-wise expansion terminates at $\xi = \xi_{l_0}$ determined by the condition

$$\max_j \left(A_{20,j}\, \xi_{l_0}^{20}\right) = 10^{-10} \tag{3.24}$$

This is an ad hoc criterion chosen by James and it is a comprimise between the need of extending as far as possible the region 1 and the need to minimize the number of terms in the series expansion.

Once the potential in the first region is found this can be extended into region 2 by analytical continuation. Suppose region 1 extends to $\xi = \xi_2$ At this point we know ψ and $\frac{\partial \psi}{\partial \xi}$. We now move outwards putting

$$\xi = \xi_1 + \eta \tag{3.25}$$

in (3.8), obtaining

$$\eta^2 \frac{\partial^2 \psi}{\partial \eta^2} + 2\eta \frac{\partial \psi}{\partial \eta} + \frac{\partial}{\partial \mu}\left[(1-\mu^2)\frac{\partial \psi}{\partial \mu}\right] + \eta^2 \rho' + 2\xi_1\left[\eta \frac{\partial^2 \psi}{\partial \eta^2} + \frac{\partial \psi}{\partial \eta} + \rho'\right] + \xi^2\left[\frac{\partial^2 \psi}{\partial \eta^2} + \rho'\right] \tag{3.26}$$

The series expansions now take the forms

$$\psi = \sum_i \sum_{j=0}^{10} \alpha_{ij}\, \eta^i P_j(\mu) \tag{3.27}$$

$$\rho' = \sum_i \sum_{j=0}^{10} \beta_{ij}\, \eta^i P_j(\mu) \tag{3.28}$$

Putting these expressions into (3.20) we will get another set of algebraic equations relating the coefficients α_{ij}, β_{ij} with the conditions

$$\alpha_{0j} = \psi_j(\xi_2) \tag{3.29}$$

$$\alpha_{1j} = \left.\frac{\partial \psi}{\partial \xi}\right)_{\xi = \xi_2} \tag{3.30}$$

The coefficients α_{ij} and β_{ij} are then determined using the same tecnique descri-

bed above for determining A_{ij} and B_{ij} relative to the region 1. Once α_j are determined we know ψ and $\frac{\partial \psi}{\partial \xi}$ at a point ξ determined by a condition similar to (3.24). Initially is $\xi_1 = \xi_0$ and the process is repeated until ξ_p is reached.

In region 3, the potential ψ and the density ρ' are not analytical functions of ξ . Indeed, for some value of polytropic index the density is discontinuos across the surface. In this region then the expansions used are of the type

$$\psi = \sum_{j=0}^{10} \psi_j(\xi) P_j(\mu) \tag{3.31}$$

$$\rho' = \sum_{j=0}^{10} \rho'_j(\xi) P_j(\mu) \tag{3.32}$$

Substituting these two into (3.8) and putting

$$\psi_j = a_j \xi^{-j-1} \tag{3.33}$$

$$\frac{da_j}{d\xi} = b_j \xi^{2j} \tag{3.34}$$

the result is

$$\frac{d}{d\xi} b_j = -\xi^{1-j} \rho'_j \tag{3.35}$$

These equations are integrated from ξ_p to ξ_e by the Runge-Kutta method with initial values for a_j, b_j determined from those of ψ and $\frac{\partial \psi}{\partial \xi}$ at $\xi = \xi_p$. The density is computed inverting (3.32) and using a similar tecnique used in region 1.

With this method the Poisson equations are reduced to a set of ordinary

differential equations which can be solved by using a Runge-Kutta method. The truncation error of this method proportional to h^4 is even related to the truncation error made on using finite series.

§ 3. Self-consistent-field methods

This method is the generalization of the well known Hartree-Fock procedure to obtain mutual consistent potential and density distribution for differential rotating polytropes. The main idea is to relate the potential and density through integral relations instead of the more customary differential equations. The boundary conditions will be then naturally incorporated in the evaluation of the integrals which can be computed numerically more accuratly than differential operators. Once this integral relations are found the already mentioned two steps can be evaluated independently, then an iteration procedure is needed to obtain self-consistency.

Let's now describe briefly the mathematical tecniques involved. The gravitational and centrifugal potentials are related to the density by the following integrals

$$\phi_g = G \int_0^r \frac{\rho(\underline{r}')}{|\underline{r} - \underline{r}'|} d\underline{r}' \tag{3.36}$$

$$\phi_c = \int_0^{\varpi} \frac{\ell^2[m(\varpi')]}{\varpi'^3} d\varpi' \tag{3.37}$$

where ϖ is the distance from the rotation axis (here (ϖ,φ,z) are used as cylindrical coordinates), ℓ the specific angular momentum and m is a Lagrangian mass coordinate defined as the fractional mass interior to the cylinder containing the element of fluid

$$m(\varpi) \equiv \frac{\int_0^{\varpi} \varpi' \int_{-\infty}^{+\infty} \rho(\varpi', z') \, d\varpi' dz'}{\int_0^{\infty} \varpi' \int_{-\infty}^{+\infty} \rho(\varpi', z') \, d\varpi' dz'} \tag{3.38}$$

The general approach to the problem is to recognize linear operator wherever

they occur, then using analytical expansions with orthonormal polynomials, the "equilibrium" and "potential" steps reduce to algebraic equations which can be solved by matrix method. For instance ϕ_g and ρ are related by mean of the linear operator

$$G \int \frac{d\underline{r}'}{|\underline{r} - \underline{r}'|} \tag{3.39}$$

whose Green's function can be expanded in terms of Legendre polynomials in the angle γ between $\underline{r}$ and $\underline{r}'$ the larger and the smaller of which we designate $r_>$ and $r_<$ respectevely

$$\frac{1}{|\underline{r} - \underline{r}'|} = \frac{1}{r_>} \sum_{n=0}^{\infty} \left(\frac{r_<}{r_>}\right)^n P_n(\cos\gamma) \tag{3.40}$$

Thus, if we expand the density in the approximate polynomial form

$$\rho(\varpi, z) = \sum_{ij} a_{ij}\, \varpi^i\, z^j \tag{3.41}$$

and the gravitational potential in the form

$$\phi_g(\varpi, z) = \sum_{kl} v_{kl}\, \varpi^k\, z^l \tag{3.42}$$

then (3.36) ensures us that we may write

$$v_{kl} = \sum_{ij} T_{ijkl}\, a_{ji} \tag{3.43}$$

where T_{ijkl} is the Green's function (3.40). Since T_{ijkl} can be evaluated once and for all, the potential (v_{kl}) can be calculated from the density (a_{ij}) by

matrix manipulation.

Using the following dimensionless quantities

$$x \equiv r/R \qquad a \equiv \varpi/R$$

$$h \equiv \ell M/J \qquad \mu \equiv \cos\theta \qquad \varsigma \equiv z/R \tag{3.44}$$

where R is the maximum radius of the star under consideration, Ostriker and Mark (1968) chose to expand the product $x^2\rho$ instead of ρ in a sphere of radius R, since that quantity appears often in integration of density over volume

$$f(x,\mu) \equiv x^2\rho(x,\mu) = \frac{3M}{4\pi R^3}\sum_{\ell=1}^{N}\sum_{m=\ell}^{N} A_{lm}\, x^{2m}\, P_{2l-2}(\mu) \tag{3.45}$$

Only even-order Legendre polynomials are used because of equatorial symmetry.

The coefficients A_{lm} must vanish if $m < l$ in order to maintain continuity at the origin. This also implies that the density assumes a finite value at the center of mass. In addition although the true density vanishes on the circumscribed sphere, the approximate density will not vanish there, thus one must add the constraint $f(1,\mu) = 0$. Under these constraints the coefficients A_{lm} are determined requiring that the mean square error between the particular form (3.45) and the more general is minimum.

Next, putting (3.40) into (3.36) and making use of (3.45) after integration we get

$$\phi_g \cong \frac{3}{2}\frac{GM}{R}\sum_{\ell=1}^{N}\sum_{m=\ell}^{N}\frac{A_{lm}\, P_{2l-2}}{(m-l+1)(4l-3)}\left(x^{2l-2} - \frac{4l-3}{2m+2l-1}\, x^{2m}\right) \tag{3.46}$$

Similarly for the centrifugal potential. Thus given the density, eq. (3.46) gives the potential in analytical form. The next step then is to compute a

new density distribution with the already determined potential and so on. The iteration is stopped when a criterion of convergence is reached. For nearly spherical stars 10-20 iterations suffice to give accuracy of 10^{-5} (Ostriker and Mark, 1968); for more flattened objects 100 iterations may be needed.

This method or modifications of it have been widely used for computing rotating configurations with arbitrary distribution of angular momentum.

Clement (1974) modified the method considering a two dimensional difference scheme for computing the Poisson equation, using a curvilinear cell with dimensions Δr and $r\Delta\vartheta$. He improved the accuracy but the convergence was still slow for flattened configurations.

Recently Stahler (1983) modified the method for treating very flattened objects such as rotating clouds. The main change occurs in evaluating the gravitational potential throughout (3.36). The integral is computed by summing over elementary toroid (see fig. 24). The cloud is divided into toroids of rectangular cross-section. The potential is computed at the "field points" (ϖ, z) located at the intersection of grid lines. The potential of a toroid of mass δM is estimated as that from a ring of the same mass located inside the toroid at (ϖ', z') ("source point"), whose expression can be given

$$\delta\phi_g(\varpi,z) = \frac{\delta M}{\pi\varpi'}\int_0^\infty J_o(y)J_o(y(\varpi/\varpi')\exp(-y\left|\frac{z'-z}{\varpi'}\right|)\,dy \qquad (3.47)$$

A proper location of the "source point" reduces the inaccuracy of using (3.47). This is made in three different steps. In the first one the torus is sliced into horizontal records, then the radius ϖ' of an infinitly ring which can replace each record is determined requiring some degree of accuracy. Since we can think that this rings from a "can" the potential will be computed

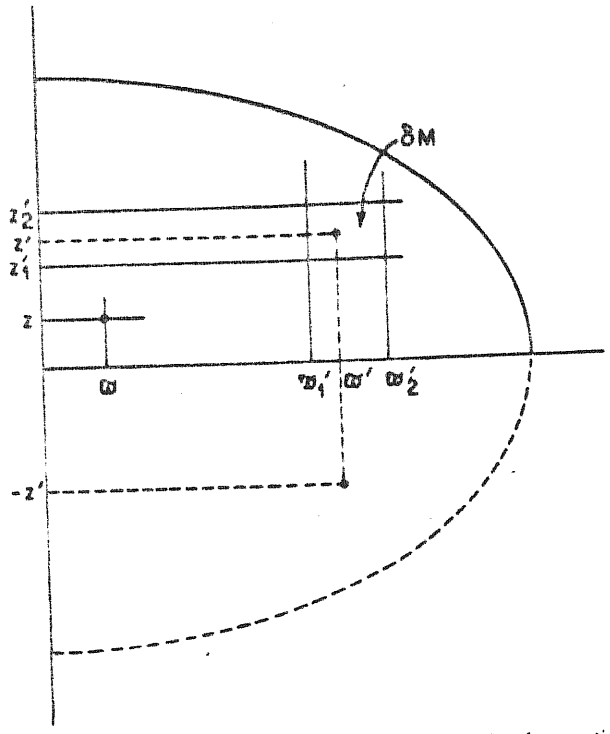

FIG. 24—The method of computing the gravitational potential. One quadrant of the cloud boundary is shown by the solid curve. The cloud is divided into toroids of rectangular cross section. We compute the potential at the field point (ϖ, z), located at the intersection of grid lines. This "point" is, of course, a ring in cross section. The potential of the toroid of mass δM is estimated as that from a ring of the same mass ("source point") located inside the toroid at (ϖ', z'). We also add the potential due to a ring in the mirror-symmetric lower half of the cloud (*dashed curve*).

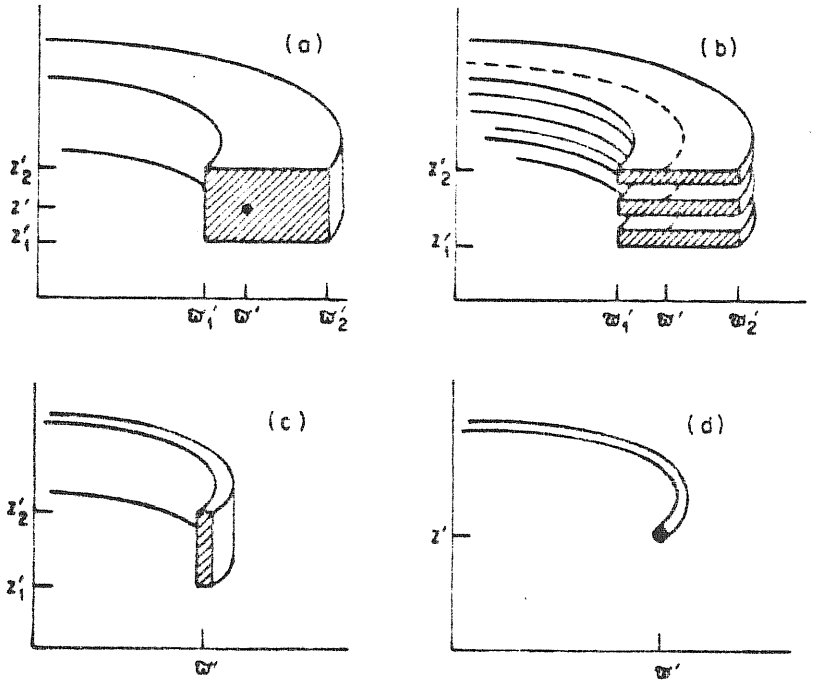

FIG. 25—Estimating the gravitational potential from the toroid. (*a*) We want to replace the toroid by a ring at (ϖ', z'). (*b*) We first slice it into flat records. Each record can be replaced by an equivalent ring (*dashed line*) of radius ϖ'. (*c*) When stacked vertically, these rings form a can. (*d*) Finally, the potential of the can is estimated as that due to a single ring at (ϖ', z'). The locations of ϖ' and z' are derived in Appendices A and B.

slicing it into rings asking for the height of the "average" ring (see fig. 25). If the "source point" are inside a cylinder sorrounding the rotation axis, then one has to use the exact formulae for a cylinder.

Although this method requires more computing time for each iteration, in the case of highly flattened equilibrium configurations it converges with fewer iterations.

Self-consistent-field method formulated using integral relations between the potential and distribution of matter has been used by Bonazzola and Schneider (1974) but as we already mentioned it does not work properly in highly relativistic regim. The problem being that these integrals contain the exterior geometry beside the distribution of matter complicating the way to obtain the solution.

A way out of this difficulty is to use the Stoeckly's method who developed a difference scheme reducing the number of points and difference equations by using few points but accurate formulae for one dimension and many points but simple formulae for the other. Indeed he used a Gauss-Legendre quadrature approximation along the μ dimension and finite difference along the r direction.

§ 4. Generalization of Stoeckly's Newtonian method.

Butterworth and Ipser (1976) modified the Henyey-type method used in Newtonian theory by Stoeckly for constructing a sequence of models with various strengths of relativity and various amount of uniform rotation or differential rotation.

In the Henyey method the differential equations of stellar structure are replaced by a set of finite difference equations. Since the equations are non linear, one starts with a trial model close to equilibrium and solves for the linear corrections. Smilarly in general relativity an initial approximation for the unknown quantities ν, ω, B, ξ, $\mathcal{R}$ or ℓ, p is obtained in one way or another. This approximation is imagined to differ by small amounts $\delta\nu$, $\delta\omega$, δB .... from the desired solution, the field equations are expanded to first order in $\delta\nu$, $\delta\omega$, δB, and a Poisson-like set of partial differential equations for $\delta\nu$, $\delta\omega$, ... is obtained, with source terms that involve only the initial approximations ν, ω, ...This set of linearized equations and another one obtained imposing boundary conditions in a way explained below are replaced by difference equations on a finite grid in the (r,μ)-plane. The difference equations are then solved for the values of $\delta\nu$, $\delta\omega$, ... , at the grid points and ν is replaced by $\nu+\delta\nu$ in the approximate solution. Next the chosen equation of state, rotation law and integrated equation of hydrostatic equilibrium are used to obtain new distributions of angular momentum and matter. These steps are iterated until convergence is achieved and the changes in quantities at the grid points drop below some desired upper limit.

The linearized field equations are obtained replacing ν, ω, B with $\nu+\delta\nu$, $\omega+\delta\omega$ and B + δB and expanding to first order in $\delta\nu$, $\delta\omega$, and δB. Thus

we get

$$B\,\delta\nu_{,rr} + \left(\frac{2B}{r} + B_{,r}\right)\delta\nu_{,r} + \frac{B}{r^2}D_\mu^2\delta\nu + \frac{(1-\mu^2)}{r^2}B_{,\mu}\,\delta\nu_{,\mu} +$$

$$\left[\left[2(1-\mu^2)r^2B^3e^{-4\nu}\left[(\omega_{,r})^2 + \frac{(1-\mu^2)}{r^2}(\omega_{,\mu})^2\right] - 4\pi Be^{2\beta}\frac{\partial}{\partial\nu}\left\{e^{-2\nu}\times\right.\right.\right.$$

$$\left.\left.\left.\times\left[\frac{(\epsilon+p)(1+v^2)}{1-v^2} + 2p\right]\right\}\right]\right]\delta\nu = -B\nu_{,rr} - \left(2\frac{B}{r} + B_{,r}\right)\nu_{,r} -$$

$$-\frac{B}{r^2}D_\mu^2\nu - \frac{(1-\mu^2)}{r^2}B_{,\mu}\nu_{,\mu} + \frac{1}{2}(1-\mu^2)r^2B^3e^{-4\nu}\left[(\omega_{,r})^2 + \frac{(1-\mu^2)}{r^2}(\omega_{,\mu})^2\right] +$$

$$+4\pi Be^{2\beta-2\nu}\left[\frac{(\epsilon+p)(1+v^2)}{1-v^2} + 2p\right] \qquad (3.48)$$

$$\delta\omega_{,rr} + \left(\frac{4}{r} + \frac{3}{B}B_{,r} - 4\nu_{,r}\right)\delta\omega_{,r} + \frac{1}{r^2}D_\mu^2\delta\omega - \left[2\mu - (1-\mu^2)\left(\frac{3}{B}B_{,\mu} - 4\nu_{,\mu}\right)\right]\frac{\delta\omega_{,\mu}}{r^2} +$$

$$+16\pi e^{2\beta-2\nu}\frac{\partial}{\partial\omega}\left[\frac{(\epsilon+p)(\Omega-\omega)}{1-v^2}\right]\delta\omega = -\omega_{,rr} - \left(\frac{4}{r} + \frac{3}{B}B_{,r} - 4\nu_{,r}\right)\omega_{,r}$$

$$-\frac{1}{r^2}D_\mu^2\omega + \left[2\mu - (1-\mu^2)\left(\frac{3}{B}B_{,\mu} - 4\nu_{,\mu}\right)\right]\frac{\omega_{,\mu}}{r^2} - 16\pi e^{2\beta-2\nu}\frac{(\epsilon+p)(\Omega-\omega)}{1-v^2}$$

$$(3.49)$$

and

$$\delta B_{,rr} + \frac{3}{r}\delta B_{,r} + \frac{1}{r^2}D_\mu^2\delta B - \frac{\mu}{r^2}\delta B_{,\mu} - 16\pi e^{2\beta-2\nu}\frac{\partial}{\partial B}(Bp)\,\delta B$$

$$= -B_{,rr} - \frac{3}{r}B_{,r} - \frac{1}{r^2}D_\mu^2 B + \frac{\mu}{r^2}B_{,\mu} + 16\pi Be^{2\beta-2\nu}p$$

$$(3.50)$$

where $\mu = \cos\theta$ and

$$D_\mu^2 f \equiv \frac{\partial}{\partial\mu}\left[(1-\mu^2)\frac{\partial f}{\partial\mu}\right] \tag{3.51}$$

The equation for the metric function ζ is already linear.

Beyond the boundary condition at the center (r = 0) and on the axis of rotation (see Cap. II) we should impose condition of asymptotic flatness at infinity. Butterworth and Ipser used expansions in power of 1/r at large radii of the metric potentials as boundary conditions. These expansions are obatined as follows. First the angular expansions are written in terms of orthonormal polynomials

$$\begin{aligned} \nu &= \sum_{\ell=0}^{\infty} \nu_{2\ell}(r)\, P_{2\ell}(\mu) \\ \omega &= \sum_{\ell=0}^{\infty} \omega_{2\ell}(r)\, P_{2\ell-1,\mu}(\mu) \\ B &= \sum_{\ell=0}^{\infty} B_{2\ell}(r)\, T_{2\ell}^{1/2}(\mu) \end{aligned} \tag{3.52}$$

where P_{21} is a Legendre polynomial and $T_{21}^{1/2}$ is a Gegenbauer polynomial (Morse and Feshbach, 1953). These polynomials are chosen since P_{21}, $P_{1,\mu}$ and $T_1^{1/2}$ are eigenfunctions of the angular parts of the operators $\underset{\sim}{\nabla}\cdot\underset{\sim}{\nabla}$, $\underset{\sim}{\nabla}\cdot r\sin\theta\underset{\sim}{\nabla}$ and $\underset{\sim}{\nabla}\cdot r^2\sin^2\theta\underset{\sim}{\nabla}$ respectevely that appears on the lhs's of the field equations. Then it is assumed that the radial parts of (3.52) have expansions in powers of 1/r at large r with leading terms given by

$$\nu \sim -\frac{M}{r} \tag{3.53}$$

$$\omega \sim \frac{2J}{r^3} \tag{3.54}$$

$$B \sim 1 \tag{3.55}$$

The actual expansions then are found substituting into the field equations the (3.52) taking into account the orthonormality relations and eqs. (3.53) -(3.55). The results are

$$\nu \sim \left\{ -\frac{M}{r} + \frac{1}{3}\tilde{B}_0 \frac{M}{r^3} + \frac{J^2}{r^4} + \left[-\tilde{B}_0^2 + \frac{1}{3}\tilde{B}_2 - 12 J^2 \right] \frac{M}{3r^5} + \cdots \right\}$$

$$+ \left\{ \frac{\tilde{\nu}_2}{r^3} - \frac{2J^2}{r^4} + \left[-3\tilde{B}_0 \tilde{\nu}_2 + \frac{16}{3}\tilde{B}_2 M + 24 J^2 M \right] \frac{1}{7r^5} + \cdots \right\} P_2(\mu) \tag{3.56}$$

$$+ \left\{ \frac{\tilde{\nu}_4}{r^5} + \cdots \right\} P_4(\mu)$$

$$\omega \sim \left\{ \frac{2J}{r^3} - \frac{6JM}{r^4} + \frac{6}{5}\left[8 - \frac{3\tilde{B}_0}{M} \right] \frac{JM^2}{r^5} + \left(\frac{10}{3}\tilde{B}_0 M - \frac{8}{3}M^3 - \frac{1}{5}\tilde{\nu}_2 \right) \frac{4J}{r^6} + \left(\cdots \right) \frac{J}{r^7} + \cdots \right\} P_{1/\mu}$$

$$+ \left\{ \frac{\tilde{\omega}_2}{r^5} + \left(\frac{9}{5}\tilde{\nu}_2 J - \frac{5}{2}\tilde{\omega}_2 M \right) \frac{1}{r^6} - \left(\cdots \right) \frac{1}{r^7} + \cdots \right\} P_{3/\mu} \tag{3.57}$$

$$+ \left\{ \frac{\tilde{\omega}_4}{r^7} + \cdots \right\} P_{5/\mu}$$

$$B \sim \left(\frac{\pi}{2} \right)^{1/2} \left(1 + \frac{\tilde{B}_0}{r^2} \right) T_0^{1/2}(\mu) + \left(\frac{\pi}{2} \right)^{1/2} \frac{\tilde{B}_2}{r^4} T_2^{1/2}(\mu) + \left(\frac{\pi}{2} \right)^{1/2} \frac{\tilde{B}_4}{r^6} T_4^{1/2}(\mu) \tag{3.58}$$

The constants $\tilde{\nu}_{2\ell}$, $\tilde{\omega}_{2\ell}$, and $\tilde{B}_{2\ell}$ are the analogues of Newtonian multipole moments. Unless $\tilde{B}_{21}$, they cannot be evaluated in terms of integrals over the matter, like in Newtonian theory because the exterior geometry acts as a source for those moments. The quantities $\tilde{B}_{21}$ can be evaluated

$$\tilde{B}_{21} = -\frac{16\pi \left(\frac{2}{\pi} \right)^{1/2}}{4\ell + 2} \int B' e^{2\beta' - 2\nu'} \rho' r'^{2\ell+3} (1-\mu^2)^{1/2} T_{2\ell}^{1/2} \, d\mu' dr' \tag{3.59}$$

Since the difficulty of evaluating $\tilde{\nu}_{2\ell}$ and $\tilde{\omega}_{2\ell}$ it is not possible to use (3.56)-(3.58) as boundary conditionsat same finite radius r . Butterworth and Ipser had the clever idea to transform the Diriclet-like boundary conditions (3.56)-(3.58) in Newmann-like ones involving the derivatives, in a way that we will illustrate here briefly. Consider the metric function ν, its angular expansion is

$$\nu(r,\mu) = \sum_{\ell=0}^{\infty} \nu_{2\ell}(r)\, P_{2\ell}(\mu) \tag{3.60}$$

and its radial derivative

$$\nu_{,r} = \sum_{\ell=0}^{\infty} \nu_{2\ell,r}(r)\, P_{2\ell}(\mu) \tag{3.61}$$

The aim now is to seek expressions for $\nu_{2\ell,r}$ in which the constants $\tilde{\nu}_{2\ell}$ are replaced by $\nu_{2\ell}(r)$. This is done simply computing the derivatives of the coefficients $\nu_{2\ell}(r)$ of (3.56) then subtructing or adding suitable terms one can replace the constants $\tilde{\nu}_{2\ell}$ with $\nu_{2\ell}(r)$. This functions then can be evaluated, as each radial function, by using a Gauss-Legendre quadrature

$$\nu_{2\ell}(r) = \frac{1}{2}(4\ell+1)\int_{-1}^{1} d\mu\, \nu(r,\mu)\, P_{2\ell}(\mu) \tag{3.62}$$

The Newmann boundary conditions (3.61) then are linearized obtaing a differential equation which will be approximated by finite difference and solved only on the right hand side of the grid. Similarly the linearized version of the boundary conditions for ω and B can be obtained. However these are more involved , since one should define new quantities by

$$\omega(r,\mu) = \sum_{\ell=0}^{\infty} \omega^{+}_{2\ell}(r)\, P_{2\ell}(\mu) \tag{3.63}$$

$$B(r,\mu) = \sum_{\ell=0}^{\infty} B_{2\ell}^{+}(r)\, P_{2\ell}(\mu) \tag{3.64}$$

before transforming the type of boundary conditions. Then one needs to connect the previosly defined quantities $\omega_{2\ell}(r)$, $B_{21}(r)$ with the new ones. It turns out that the following sets of equations have to be solved

$$\omega_{2m}^{+}(r) = 2\left[\frac{(2m+1)(m+1)}{4m+3}\,\omega_{2m}(r) - \frac{(2m-1)m}{4m-1}\,\omega_{2m-2}(r)\right] + \frac{4m+1}{2}\sum_{\ell=0}^{\infty}\omega_{2\ell}^{+}(r)\int \mu^{2} P_{2\ell}\, P_{2m}\, d\mu \tag{3.65}$$

$$B_{2m}^{+}(r) = \frac{4m+1}{2}\sum_{\ell=0}^{\infty} B_{2\ell}(r)\int_{-1}^{1} T_{2\ell}^{\frac{1}{2}}\, P_{2m}\, d\mu \tag{3.66}$$

With this method the computer essentially decides on the values of the multiple moments in a manner consistent with the field equations.

The difference equations are computed on a finite grid in the (r,μ)-plane. The grid consists of a chosen number N of radial spokes emanating from the origin at the Gauss-Legendre quadrature values $\mu_1 = 0, \mu_2, \cdots \mu_N$. A chosen number I of grid points are uniformly spaced at chosen radial intervals Δr along each spoke.

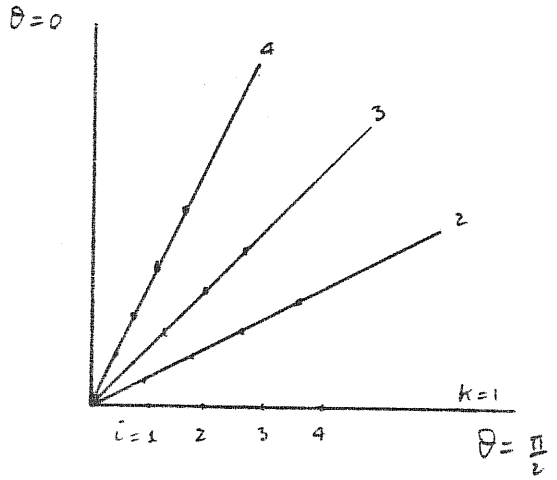

The radial derivative are approximated using central formulae of the type

$$f_{,r}(r_i,\mu_\kappa) \approx \frac{f_{i+1,\kappa} - f_{i-1,\kappa}}{2\Delta r}$$

$$f_{,rr}(r_i,\mu_\kappa) \approx \frac{f_{i-1,\kappa} - 2f_{i,\kappa} + f_{i+1,\kappa}}{\Delta r^2}$$

whereas the angular derivatives are approximated with sufficient accuracy by using the Gauss-Legendre quadrature

$$f(r_i,\mu_\kappa) \approx \sum_{m=1}^{N} B_{\kappa m} f(r_i,\mu_m)$$

$$f_{,\mu}(r_i,\mu_\kappa) \approx \sum_{m=1}^{N} F_{\kappa m} f(r_i,\mu_m)$$

$$D_\mu^2 f(r_i,\mu_\kappa) \approx \sum_{m=1}^{N} G_{\kappa m} f(r_i,\mu_m)$$

where

$$B_{km} \equiv \sum_{\ell=0}^{N-1} \frac{4\ell+1}{2} H_m P_{2\ell}(\mu_m) P_{2\ell}(\mu_\kappa)$$

$$F_{km} \equiv \sum_{\ell=1}^{N-1} \frac{1}{2}(4\ell+1) H_m P_{2\ell,\mu}(\mu_\kappa) P_{2\ell}(\mu_m)$$

$$G_{km} \equiv -\sum_{\ell=1}^{N-1} \ell(2\ell+1)(4\ell+1) H_m P_{2\ell}(\mu_\kappa) P_{2\ell}(\mu_m)$$

are independent of the particular function to approximate and are computed throughout the weightining functions H_m which are tabulated (see e.g. Kopal,1961). Here H_m, for $m \geq 2$, are to be assigned twice their usual values , since only quadrature points at non negative μ are used.

When an equation of state, a rotation law and an initial approximation close to equilibrium are specified, the difference equations are solved by Gaussian-elimination tecniques for getting $\delta\nu$. Then ν is repalced with $\nu+\delta\nu$ and this value is used to integrate the hydrostatic equilibrium equation to get new values of $\mathcal{R}$ and p. These new quantities are used to solve (3.49) for getting δw and recompute $\mathcal{R}$ and p as before. Solve eq. (3.50) to obtain

new B, then use eq. (2.8) to compute ς and recompute $\mathcal{R}$ and p as before. The iteration is repeated until the process converges.

A modification of this method has been used to construct a numerical code able to follow the full relativistic dynamical collapse into a black hole of an axisymmetric configurations by Smith (1983). He used as initial condition the models constructed by Butterworth and Ipser.

CONCLUSIONS

The results and theorems presented in this thesis are those we think are important to know for constructing equilibrium models in general. The sequence we would like to compute is that of self-gravitating torii in the framework of general relativity. Since the non-linearity of the Einstein equations this has to be done numerically. We will apply the method used by Butterworth and Ipser with suitable modifications in order to take into account of presence of horizon for instance. As initial approximation for the field we will choose the Kerr metric supposing that the torus is only weakly self-gravitating. Solving the Einstein's equations for the corrections to the metric functions we will iterate between matter distribution and field. When convergence is reached we start again the iteration increasing the mass of the torus. This can be done for different values of constant angular momentum. In this way we may construct two sequences: one with fixed constant angular momentum and different masses of the torus and another with fixed mass and different values of ~~the mass~~ constant angular momentum.

REFERENCES

M.A.Abramowicz, Astrophys. Letters, 7, 73, 1970.

M.A.Abramowicz, Acta Astron., 24, 45, 1974.

M.A.Abramowicz, Ap.J., 254, 748, 1982.

M.A.Abramowicz, M.Calvani, and L.Nobili, Nature, 302, 597, 1983.

M.A.Abramowicz, and R.Wagoner, Ap.J., 204, 896, 1976.

J.M.Bardeen, Ap.J., 161, 103, 1970a.

J.M.Bardeen, Ap.J., 162, 71, 1970b.

J.M.Bardeen, Ap.J., 167, 425, 1971.

J.M.Bardeen, "Rapidly Rotating Stars, Disks and Black Holes", in Black Holes eds. B.De Witt and C.De Witt, Gordon and Breach, New York, 1973.

J.M.Bardeen, B.Carter, and S.W.Hawking, Comm.Math.Phys., 31, 181, 1973.

J.M.Bardeen and R.Wagoner, Ap.J., 167, 359, 1971.

P.Bodenheimer and J.Ostriker, Ap.J., 180, 159, 1973.

S.Bonazzola and J.Schneider, Ap.J., 191, 173, 1974.

R.H.Boyer, Proc.Cambr.Phil.Soc., 61, 527, 1965.

E.M.Butterworth, Ap.J., 204, 561, 1976.

E.M.Butterworth, Ap.J., 231, 219, 1979.

E.M.Butterworth and J.R.Ipser, Ap.J., 204, 200, 1976.

E.M.Butterworth and J.R.Ipser, Ap.J.Letters, 200, L103, 1975.

B.Carter, "General Theory of Stationary Black Hole States", in Black Holes, eds. B.De Witt and C.De Witt, Gordon and Breach, New York, 1973.

B.Carter, "The general Theory of the Mechanical, electromagnetic and Thermodynamic Properties of Black Holes", in General relativity, An Einstein Centenary Survey, eds. S.W.Hawking and W.Israel, Cambridge University Press, Cambridge, 1979.

S.Chandrasekhar, Ap.J., 140, 417, 1964.

S.Chandrasekhar, Ap.J., 142, 1513, 1965.

S.Chandrasekhar, Ap.J., 147, 334, 1967.

S.Chandrasekhar, Ap.J., 161, 561, 1970.

S.Chandrasekhar, Ap.J., 167, 447, 1971.

S.Chandrasekhar and J.L.Friedman, Ap.J., 175, 379, 1972.

S.Chandrasekhar and J.C.Miller, Mon.Not.R.astr.Soc., 167, 63, 1974.

M.J.Clement, Ap.J., 194, 709, 1974.

F.W.Dyson, Phil.Trans.Roy.Soc.London, 184, 43-95, 1041-1107, 1893.

B.K.Harrison, K.S.Thorne, M.S.Wakano, and J.A.Wheeler, "Gravitation Theory and Gravitational Collapse", 1965.

J.B.Hartle, Ap.J., 150, 1005, 1967.

J.B.Hartle and D.W Sharp, Phys.Rew.Lett., 27, 529, 1965.

J.B.Hartle and D.W Sharp, Ap.J., 147, 317, 1967.

J.B.Hartle and K.S.Thorne, Ap.J., 153, 807, 1968.

S.W.Hawking, "The Event Horizon", in Black Holes, eds. B.De Witt and C.De Witt, Gordon and Breach, New York, 1973.

S.W.Hawking and G.F.R.Ellis, "The Large Scale Structure of Space-Time", Cambridge University Press, Cambridge, 1973.

R.A.James, Ap.J., 140, 552, 1964.

Z.Kopal, "Numerical Analysis", 2d ed. Chapman and Hall, London, 1961.

P.S.Laplace, "Memorie sur la thèorie de l'anneau de Saturne", Mem.Acad.Sci., 1789.

L.Lichtenstein, "Gleichgewichtsfigureu Rotierender Flüssgkeiten", Springer-Verlag, Berlin, 1933.

L.Lindblom and S.L.Detweiler, Ap.J., 211, 565, 1977.

J.C.Maxwell, "On the Stability of the Motions in Saturn's Rings", Admas Prize Essay reprinted in Scientific Papers of J.C.Maxwell, Cambridge University Press, Cambridge, 1859.

B.D.Miller, Ap.J., 181, 497, 1973.

J.C.Miller, Mon.Not.R.astr.Soc., 179, 483, 1977.

P.M.Morse and H.Feshbach, "Methods of Theoretical Physics", MacGraw-Hill, New York, 1953.

T.Nakamura, Progr. of Theor. Phys., 65, 1876, 1981.

J.Ostriker, Ap.J., 140, 1056, 1964a.

J.Ostriker, Ap.J., 140, 1067, 1964b.

J.Ostriker and P.Bodenheimer, 180, 159, 1973.

J.Ostriker and J.W.Mark, Ap.J.,151, 1075, 1968.

B.Paczynski, private communication.

J.C.B.Papaloizou and J.E.Pringle, Mon.Not.R.astr.Soc., 208,721, 1984.

H.Poincarè, summarized in F.Tisserand, "Mecnique Cleste", Gauthier-Villars, Paris, 1891.

W.H.Press and S.A.Teukolsky, Ap.J., 181, 513, 1973.

G.Randers, Ap.J., 92, 235, 1942.

P.H.Roberts, Ap.J., 136, 1108, 1962.

M.Rees, Ann.Rev.Astron.Astrophys., 1984.

I.G.Shakhman, Sov.Astron., 27, 129, 1983.

L.Smarr, Phys.Rev.Letters, 30, 71, 1973.

A.L.H.Smith, D.Phil.Thesis, University of Oxford, Oxford, 1983.

S.W.Sthahler, Ap.J., 268, 155, 1983.

R.Stoeckly, Ap.J., 142, 208, 1965.

J.L.Tassoul, "Theory of Rotating Stars", Princeton University Press, Princeton, 1978.

S.Tsuruta and A.G.W.Cameron, Canadian J.Phys., 44, 1895, 1966.

C.W.Will,Ap.J., 191, 521, 1974.

C.W.Will, Ap.J., 196, 41, 1975.

J.R.Wilson, Ap.J., 176, 195, 1972.

C.-Y.Wong, Ann.Phys.(N.Y.), 77, 279, 1973.

C.-Y.Wong, Ap.J., 190, 675, 1974.